

CAUSAL NETWORK INFERENCE BY OPTIMAL CAUSATION ENTROPY*

JIE SUN[†], DANE TAYLOR[‡], AND ERIK M. BOLLE[§]

Abstract. The broad abundance of time series data, which is in sharp contrast to limited knowledge of the underlying network dynamic processes that produce such observations, calls for an general and efficient method of causal network inference. Here we develop mathematical theory of Causation Entropy, a model-free information-theoretic statistic designed for causality inference. We prove that for a given node in the network, the collection of its direct causal neighbors forms the *minimal set of nodes that maximizes Causation Entropy*, a result we refer to as the *Optimal Causation Entropy Principle*. This principle guides us to further develop computational and data efficient algorithms for causal network inference. Analytical and numerical results for Gaussian processes on large random networks highlight that inference by Optimal Causation Entropy outperforms previous leading methods including Conditional Granger Causality and Transfer Entropy. Interestingly, our numerical results also indicate that the number of samples required for accurate inference depends strongly on network characteristics such as the density of links and information diffusion rate and not on the number of nodes.

Key words. causal network inference, optimal causation entropy, stochastic network dynamics

AMS subject classifications. 37N99, 62B10, 94A17

1. Introduction. Research of dynamic processes on large-scale complex networks has attracted considerable interest in recent years with exciting developments in a wide range of disciplines in social, scientific, engineering, and medical fields [41, 42, 64]. One important line of research focuses on exploring the role of network structure in determining the dynamic properties of a system [4, 13, 14, 15, 21, 47, 58, 67] and utilizing such knowledge in controlling network dynamics [11, 60] and optimizing network performance [10, 32, 43, 48, 62]. In many applications such as the study of neuronal connectivity or gene interactions, however, it is nearly impossible to directly identify the network structure without severely interfering with the underlying system whereas time series measurements of the individual node states are often more accessible [59]. From this perspective, it is crucial to reliably infer the network structure that shapes the dynamics of a system from time series data. It is essential that one accounts for directed “cause and effect” relationships, which often offer deeper insight than non-directed relationships (e.g., correlations) [46, 53, 57]. In particular, causal network inference has shown to be a central problem in the research of social perception [29], epidemiological factors [49], neural connectivity [8, 9], economic impacts [28], and basic physical relationships of climatological events [51, 52]. Evidently, understanding causality is a necessary and important precursor step towards the goal of effectively controlling and optimizing system dynamics (e.g., medical intervention of biological processes and policy design for economic growth and social development).

In a network dynamic process involving a large number of nodes, causal relationships are inherently difficult to infer. For example, the fact that a single node can potentially be influenced by many (if not all) others through network interactions

*This work was funded by ARO Grant No. 61386-EG (J.S and E.M.B), and NSF Grant No. DMS-1127914 through the Statistical and Applied Mathematical Sciences Institute (D.T.).

[†]Department of Mathematics, Clarkson University, Potsdam, NY 13699 (sunj@clarkson.edu).

[‡]Statistical and Applied Mathematical Sciences Institute, Research Triangle Park, NC 27709; Department of Mathematics, University of North Carolina, Chapel Hill, NC 27599.

[§]Department of Mathematics, Clarkson University, Potsdam, NY 13699.

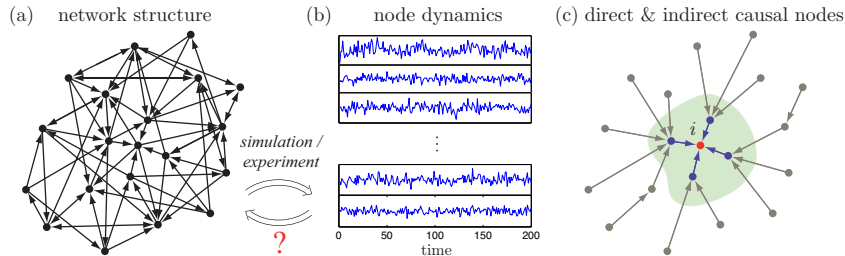


FIG. 1.1. *Network dynamics, time series, and the causal network inference problem.* Modern scientific approaches such as simulation, experiments, and data mining have produced an abundance of high-dimensional time series data describing dynamic processes on complex networks (a→b). Given empirical observations, an important problem is to infer the causal network structure that underlies the observed time series. As shown in (c), for each node i , the goal is to identify the nodes that directly cause its dynamics (nodes in shaded region), while pruning away the nodes that do not (nodes outside the shaded region), thus recovering the direct links to node i in the causal network.

makes it challenging to uncover the direct causal nodes from indirect and erroneous ones (see Fig. 1.1 for illustration). Granger recognized the crucial role played by conditioning and proposed that a causal relationship should satisfy two basic principles [23, 24]:

- (i) The cause should occur before the effect;
- (ii) The cause should contain information about the caused that is not available otherwise.

A relationship that fulfills both requirements is unambiguously defined as causal. In practice, although the first requirement is straightforward to examine when temporal information of the data is available, it is difficult to check the second as it involves the consideration of virtually *all* other nodes in the network. In practice, tradeoffs are often made, by either restricting to small-scale networks with no time delay and just a handful of variables [26, 61], or partially removing the second requirement therefore reducing the accuracy of network inference [65]. Inferring large-scale networks from time series data therefore remains to be a relatively open problem [35, 59].

Information-based causality inference approaches overcome the model-dependent limitation often seen in traditional methods such as the Granger causality test [23, 24]. In particular, Schreiber proposed Transfer Entropy as a measure of information flow, or effective coupling, between two processes regardless of the actual functional relationship between them [54]. The Transfer Entropy from process Y to X measures the uncertainty reduction of the future states of X as a result of knowing the past of Y given that the past of X is already known, and is essentially the mutual information between the future of X and history of Y *conditioning* on the history of X [31, 44]. Because of its ability to associate time directionality with coupling, Transfer Entropy has quickly started to gain popularity in a broad range of disciplines including bioinformatics, neuroscience, climatology and others, as a practical tool to infer effective pairwise coupling that underlie complex dynamic processes [6, 65]. However, Transfer Entropy, which was introduced specifically for detecting the directionality of information flow between two processes, has been shown to have fundamental limitations when applied to the inference of networks [56, 61]. In particular, without proper conditioning, inference based on Transfer Entropy tends to produce systematic errors due to, for example, the effects of indirect influences and dominance of neighbors [61].

In this paper we develop theory of Causation Entropy—a type of conditional

mutual information designed for causal network inference. In particular, we prove the Optimal Causation Entropy Principle for general stochastic processes: the set of nodes that directly cause a given node is the unique minimal set of nodes that maximizes Causation Entropy. This principle allows us to convert the problem of causality inference into the optimization of Causation Entropy. We further show that this optimization problem, which appears to be combinatorial, can in fact be solved by simple greedy algorithms, which are both computationally efficient and data efficient. We confirm the effectiveness of the proposed algorithms through analytical and numerical investigations of Gaussian processes on various network types including trees, loops, and random networks. Somewhat surprisingly, our results suggest that it is the density of links and information diffusion rate rather than the number of nodes in a network that determines the minimal sample size required for accurate inference.

2. Stochastic Process and Causal Network Inference. We begin by introducing a theoretical framework for inferring causal networks from high-dimensional time series. This framework is general in that it is applicable to both linear and non-linear systems with or without added noise.

Consider a network (graph) $\mathcal{G} = (\mathcal{V}, \mathcal{E})$, with $\mathcal{V} = \{1, 2, \dots, n\}$ being the set of nodes and $\mathcal{E} \subset \mathcal{V} \times \mathcal{V} \times \mathbb{R}$ being the set of weighted links (or edges), where $(j, i, e_{ij}) \in \mathcal{E}$ iff $j \rightarrow i$ with link weight e_{ij} . The *adjacency matrix* $A = [A_{ij}]_{n \times n}$ is defined as

$$(2.1) \quad A_{ij} = \begin{cases} e_{ij}, & \text{if } j \rightarrow i \text{ with weight } e_{ij}; \\ 0, & \text{otherwise.} \end{cases}$$

We use $\chi_0(A)$ to denote the corresponding unweighted adjacency matrix defined entry-wise by $\chi_0(A)_{ij} = 1$ iff $A_{ij} \neq 0$ and $\chi_0(A)_{ij} = 0$ iff $A_{ij} = 0$. We define the set of *direct causal neighbors* of i as

$$(2.2) \quad N_i = \{j | A_{ij} \neq 0\} = \{j | \chi_0(A)_{ij} = 1\}.$$

For a subset of nodes $I \subset \mathcal{V}$, we similarly define its set of direct causal neighbors as

$$(2.3) \quad N_I = \cup_{i \in I} N_i.$$

We consider stochastic network dynamics in the following form (for each node i)

$$(2.4) \quad X_t^{(i)} = f_i(A_{i1}X_{t-1}^{(1)}, A_{i2}X_{t-1}^{(2)}, \dots, A_{ij}X_{t-1}^{(j)}, \dots, A_{in}X_{t-1}^{(n)}, \xi_t^{(i)})$$

where $X_t^{(i)} \in \mathbb{R}^d$ is a random variable representing the state of node i at time t , $\xi_t^{(i)} \in \mathbb{R}^d$ is the random fluctuation on node i at time t , and $f_i : \mathbb{R}^{d \times (n+1)} \rightarrow \mathbb{R}^d$ models the functional dependence of the state of node i on the past states of nodes j with $A_{ij} \neq 0$. Note that other than the noise term $\xi_t^{(i)}$, the state $X_t^{(i)}$ only depends (stochastically) on the past states of its direct causal neighbors, $X_{t-1}^{(j)}$ ($j \in N_i$).

For a subset $K = \{k_1, k_2, \dots, k_q\} \subset \mathcal{V}$, we define

$$(2.5) \quad X_t^{(K)} \equiv [X_t^{(k_1)}, X_t^{(k_2)}, \dots, X_t^{(k_q)}]^\top.$$

If $K = \mathcal{V}$, we simplify the notation and denote

$$(2.6) \quad X_t \equiv X_t^{(\mathcal{V})} = [X_t^{(1)}, X_t^{(2)}, \dots, X_t^{(n)}]^\top.$$

2.1. Problem of Causal Network Inference and Challenges. Given quantitative observations of the dynamic states of individual nodes, often in the form of time series, a central problem is to infer its (causal) system dynamics, which involves the inference of (1) the causal network topology, $\chi_0(A)$; (2) the link weights, $\{e_{ij}\}$; and (3) the specific forms of functional dependence between nodes, $\{f_i\}$. Because each of these steps is challenging, we focus on the first step: inferring the causal network topology $\chi_0(A)$, which serves as the skeleton of the actual network dynamics. See Fig. 1.1 as a schematic illustration. In particular, the problem of causal network inference can be casted mathematically as:

$$(2.7) \quad \begin{cases} \text{Given:} & \text{Samples of the node states } x_t^{(i)} \ (i = 1, 2, \dots, n; \ t = 1, 2, \dots, T). \\ \text{Goal:} & \text{Infer the structure of the underlying causal network,} \\ & \text{i.e., find } \operatorname{argmin}_A \|\chi_0(A) - \hat{A}\|_0, \text{ where } \|M\|_0 \equiv \sum_{i,j} |M_{ij}|^0. \end{cases}$$

One key challenge is that in many applications, the number of nodes n is often *large* (usually hundreds at least), but the sample size T is much smaller than needed for reliable estimation of the $(n \times d)$ -dimensional joint distribution. We propose that a practical causation inference method should fulfill the following three principles:

1. *Model-free.* The method should not rely on assumptions about either the form or parameters of a model that underlie the process.
2. *Computational Efficient.* The method should be computationally efficient.
3. *Data Efficient.* The method should achieve high accuracy with relatively small number of samples (i.e., convergence in probability needs to be fast).

In this paper we address the model-free requirement by utilizing information-theoretic measures, and in particular, by using Causation Entropy. On the other hand, our theoretical developments of the Optimal Causation Entropy Principle enables us to develop algorithms that are both computationally efficient and data efficient.

2.2. Markov Assumptions. We will study the system in a probabilistic framework under Markov assumptions. Extension of the main results to general stochastic processes with finite or vanishing memory are possible but are left for future work. Unless specified otherwise, we make the following assumptions regarding the conditional distributions $p(\cdot|\cdot)$ arising from the stochastic network dynamics in Eq. (2.4). For every node $i \in \mathcal{V}$ and time indices t, t' :

$$(2.8) \quad \begin{cases} (1) \text{ Temporally Markov:} \\ \quad p(X_t|X_{t-1}, X_{t-2}, \dots) = p(X_t|X_{t-1}) = p(X_{t'}|X_{t'-1}). \\ (2) \text{ Spatially Markov:} \\ \quad p(X_t^{(i)}|X_{t-1}) = p(X_t^{(i)}|X_{t-1}^{(N_i)}). \\ (3) \text{ Minimally Markov (with respect to time and space):} \\ \quad p(X_t^{(i)}|X_{t-1}, X_{t-2}, \dots) \neq p(X_t^{(i)}|X_{t-1}^{(K)}) \text{ if } K \not\supset N_i. \end{cases}$$

Throughout the paper, the relationship between two probability density functions p_1 and p_2 are denoted as “ $p_1 = p_2$ ” iff they equal *almost everywhere*, and “ $p_1 \neq p_2$ ” iff there is a set of positive measure on which the two functions do not equal.

In Eq. (2.8), condition (1) states that the underlying stochastic process is a (classical) Markov process, which ensures that the causal dependences between nodes, which are captured by conditional probabilities, are stationary. Condition (2) is often referred to as the (local) Markov property [38], which we call Spatially Markov here

to differ from Temporally Markov. This condition guarantees that in determining the future state of a node, if knowledge about the past states of all its direct causal neighbors N_i [as defined in Eq. (2.2)] is given, information about the past of any other node becomes irrelevant. Finally, condition (3) establishes that the set of causal neighbors N_i is the *unique* and *minimal* set of nodes that directly influence node i : any set $K \not\supset N_i$ does not capture the full conditional dependence of node i on the network.

Note that the conditional independence of two random variables X and Y conditioning on Z can also be denoted simply by $(X \perp\!\!\!\perp Y \mid Z)$, i.e.,

$$(2.9) \quad (X \perp\!\!\!\perp Y \mid Z) \iff p(X|Y, Z) = p(X|Z).$$

The following results regarding conditional independence will be useful in later sections and are direct consequences of the basic axioms of probability theory [25, 38, 46]:

$$(2.10) \quad \begin{cases} \text{Symmetry: } (X \perp\!\!\!\perp Y \mid Z) \iff (Y \perp\!\!\!\perp X \mid Z). \\ \text{Decomposition: } (X \perp\!\!\!\perp YW \mid Z) \implies (X \perp\!\!\!\perp Y \mid Z). \\ \text{Weak union: } (X \perp\!\!\!\perp YW \mid Z) \implies (X \perp\!\!\!\perp Y \mid ZW). \\ \text{Contraction: } (X \perp\!\!\!\perp Y \mid Z) \wedge (X \perp\!\!\!\perp W \mid ZY) \implies (X \perp\!\!\!\perp YW \mid Z). \\ \text{Intersection: } (X \perp\!\!\!\perp Y \mid ZW) \wedge (X \perp\!\!\!\perp W \mid ZY) \implies (X \perp\!\!\!\perp YW \mid Z). \end{cases}$$

Here “ \wedge ” denotes the logical operations “and” (the symbol “ \vee ” is used later for “or”), and YW denotes a joint random variable of Y and W .

2.3. Causation Entropy as an Information-Theoretic Measure. We review several fundamental concepts in information theory, leading to Causation Entropy, a model-free information-theoretic statistic that can be used to infer direct causal relationships [61].

Originally proposed by Shannon as a measure of uncertainty and complexity, the (differential) *entropy* of a continuous random variable $X \in \mathbb{R}^n$ is defined as [12, 55]¹

$$(2.11) \quad h(X) = - \int p(x) \log p(x) dx,$$

where $p(x)$ is the probability density function of X . The joint and conditional entropies between two random variables X and Y are defined as [also see Fig. 2.1(a)]

$$(2.12) \quad \begin{cases} \text{Joint entropy: } h(X, Y) \equiv h(Y, X) \equiv - \int p(x, y) \log p(x, y) dx dy. \\ \text{Conditional entropies: } \begin{cases} h(X|Y) \equiv - \int p(x, y) \log p(x|y) dx dy; \\ h(Y|X) \equiv - \int p(x, y) \log p(y|x) dx dy. \end{cases} \end{cases}$$

For more than two random variables, the entropies are similarly defined (as above) by grouping the variables into two classes, one acting as X and the other as Y .

The *mutual information* between two random variables X and Y (conditioning on Z) can be interpreted as a measure of the deviation from independence between X and Y (conditioning on Z). The corresponding unconditioned and conditional mutual information are defined respectively as

$$(2.13) \quad \begin{cases} \text{Mutual information: } I(X; Y) \equiv h(X) - h(X|Y) \equiv h(Y) - h(Y|X). \\ \text{Conditional mutual information:} \\ \quad I(X; Y|Z) \equiv h(X|Z) - h(X|Y, Z) \equiv h(Y|Z) - h(Y|X, Z). \end{cases}$$

¹We follow the convention in Ref. [12] to use $h(\cdot)$ for the entropy of a continuous random variable and reserve $H(\cdot)$ for the entropy of a discrete random variable. In the discrete case, we need to replace the integral by summation and probability density by probability mass function in the definition.

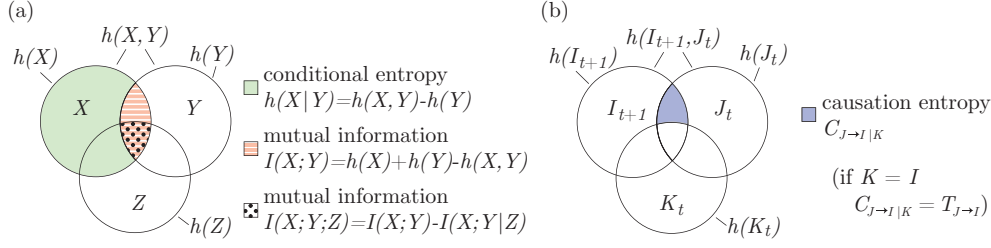


FIG. 2.1. Venn-like diagrams for information-theoretic measures. (a) Visualization of the relationships between entropy, conditional entropy, and mutual information. (b) Visualization of the relationships between conditional entropy, Causation Entropy, and Transfer Entropy. In the picture of (b), letters I , J , and K are used to denote $X^{(I)}$, $X^{(J)}$, and $X^{(K)}$, respectively.

The mutual information among three variables X , Y , and Z is defined as

(2.14)

$$I(X; Y; Z) \equiv I(X; Y) - I(X; Y|Z) \equiv I(Y; Z) - I(Y; Z|X) \equiv I(X; Z) - I(X; Z|Y),$$

The mutual information between two variables is always nonnegative, $I(X; Y) \geq 0$, with equality if and only if X and Y are independent. Similarly, $I(X; Y|Z) \geq 0$, with equality if and only if X and Y are independent when conditioned on Z . Interestingly, for three or more variables, such an inequality does not hold: the mutual information $I(X; Y; Z)$ can be either positive, negative or zero [40]. Figure 2.1(a) visualizes the relationships between entropy, conditional entropy, and mutual information.

To measure the directionality of information flow between two random processes, Schreiber proposed a specific type of conditional mutual information called *Transfer Entropy* [54]. For the stochastic process defined by Eq. (3.1), the Transfer Entropy from j to i (with time shift $\tau = 1$) can be expressed as (assuming the limit exists)

$$(2.15) \quad T_{j \rightarrow i} \equiv \lim_{t \rightarrow \infty} [h(X_{t+1}^{(i)} | X_t^{(i)}) - h(X_{t+1}^{(i)} | X_t^{(i)}, X_t^{(j)})],$$

where $h(\cdot|\cdot)$ denotes conditional entropy [12]. Since the conditional entropy $h(X_{t+1}^{(i)} | X_t^{(i)})$ measures the uncertainty of $X_{t+1}^{(i)}$ given information about $X_t^{(i)}$ and $h(X_{t+1}^{(i)} | X_t^{(i)}, X_t^{(j)})$ measures the uncertainty of $X_{t+1}^{(i)}$ given information about both $X_t^{(i)}$ and $X_t^{(j)}$, the Transfer Entropy $T_{j \rightarrow i}$ can be interpreted as the *reduction of uncertainty* about future states of $X^{(i)}$ when the current state of $X^{(j)}$ is provided *in addition to that of* $X^{(i)}$.

Networks of practical interest inevitably contain (many) more than two nodes. As we will show later, without appropriate conditioning Transfer Entropy fails to distinguish between direct and indirect causality in networks. To overcome the pairwise limitation of Transfer Entropy, we define *Causation Entropy*. The relationships between entropy, Transfer Entropy and Causation Entropy are illustrated in Fig 2.1(b).

DEFINITION 2.1 (Causation Entropy [61]). *The Causation Entropy from the set of nodes J to the set of nodes I conditioning on the set of nodes K is defined as*

$$(2.16) \quad C_{J \rightarrow I|K} = \lim_{t \rightarrow \infty} [h(X_{t+1}^{(I)} | X_t^{(K)}) - h(X_{t+1}^{(I)} | X_t^{(K)}, X_t^{(J)})]$$

(assuming that the limit exists), where I, J, K are all subset of $\mathcal{V} = \{1, 2, \dots, n\}$. In particular, if $J = \{j\}$ and $I = \{i\}$, we simplify the notation as $C_{j \rightarrow i|K}$. If the conditioning set $K = \emptyset$, we often omit it and simply write $C_{J \rightarrow I}$.

REMARK 2.1. *Causation Entropy is a natural generalization of Transfer Entropy from measuring pairwise causal relationships to network relationships of many variables. In particular, if $j \in K$, then the Causation Entropy $C_{j \rightarrow i|K} = 0$ as j does not carry extra information (compared to that of K). On the other hand, if $K = \{i\}$, Causation Entropy recovers Transfer Entropy, i.e.,*

$$(2.17) \quad C_{j \rightarrow i|i} = T_{j \rightarrow i}.$$

Interestingly, in this framework we see that Transfer Entropy assumes that nodes are self-causal, whereas Causation Entropy relaxes this assumption. Preliminary exploration of the differences between the two measures can be found in Ref. [61].

REMARK 2.2. *It seems plausible to conjecture that if two subsets of the nodes satisfy $K_1 \subset K_2$, then $C_{j \rightarrow i|K_1}$ would be no less than $C_{j \rightarrow i|K_2}$. We remark that this statement about monotonicity is false (see the two examples below).*

Example 1. *Consider the stochastic process*

$$(2.18) \quad X_t^{(1)} = X_{t-1}^{(2)} + X_{t-1}^{(3)}$$

where $X_t^{(k)}$ are i.i.d Bernoulli variables: $P(X_t^{(k)} = 0) = P(X_t^{(k)} = 1) = 0.5$ ($k = 2, 3$). Let $i = 1$, $j = 2$, $K_1 = \emptyset$ and $K_2 = \{3\}$. It follows that

$$(2.19) \quad \begin{cases} C_{2 \rightarrow 1|\emptyset} = \frac{3}{2} \log 2 - \log 2 = \frac{1}{2} \log 2 \\ C_{2 \rightarrow 1|\{3\}} = \log 2 - 0 = \log 2 \end{cases} \Rightarrow C_{2 \rightarrow 1|\emptyset} < C_{2 \rightarrow 1|\{3\}}.$$

Example 2. *Consider the stochastic process*

$$(2.20) \quad X_{t+1}^{(1)} = X_t^{(3)}, \quad X_{t+1}^{(2)} = X_t^{(3)},$$

where $X_t^{(3)}$ are Bernoulli variables with $P(X_t^{(3)} = 0) = P(X_t^{(3)} = 1) = 0.5$. Let $i = 1$, $j = 2$, $K_1 = \emptyset$ and $K_2 = \{3\}$. It follows that

$$(2.21) \quad \begin{cases} C_{2 \rightarrow 1|\emptyset} = \log 2 - 0 = \log 2 \\ C_{2 \rightarrow 1|\{3\}} = 0 - 0 = 0 \end{cases} \Rightarrow C_{2 \rightarrow 1|\emptyset} > C_{2 \rightarrow 1|\{3\}}.$$

The seemingly paradoxical observation that $C_{j \rightarrow i|K_1}$ can either be larger or smaller than $C_{j \rightarrow i|K_2}$ despite the fact that $K_1 \subset K_2$ can be understood as follows: When $K_1 \subset K_2$, $C_{j \rightarrow i|K_1} - C_{j \rightarrow i|K_2}$ corresponds to the mutual information among the three variables $X_{t+1}^{(i)}|X_t^{(K_1)}$, $X_{t+1}^{(i)}|X_t^{(j)}$ and $X_{t+1}^{(i)}|X_t^{(K_2-K_1)}$ (see Fig. 2.1). Contrary to the two-variable case where mutual information is always nonnegative, the mutual information among three (or more) variables can either be positive, negative or zero [40].

2.4. Theoretical Properties of Causation Entropy and the Optimal Causation Entropy Principle. In the following we show that analysis of Causation Entropy leads to exact network inference for the network stochastic process given by Eq. (2.4) subject to the Markov assumptions in Eq. (2.8).

We start by exploring basic analytical properties of Causation Entropy, which is presented as Theorem 2.2 and also summarized in Fig. 2.2.

THEOREM 2.2 (Basic Analytical Properties of Causation Entropy). *Suppose that the network stochastic process given by Eq. (2.4) satisfies the Markov assumptions in Eq. (2.8). Let $I \subset \mathcal{V}$ be a set of nodes and N_I be the set of its direct causal neighbors. Consider two sets of nodes $J \subset \mathcal{V}$ and $K \subset \mathcal{V}$. The following results hold:*

- (a) (*Redundancy*) If $J \subset K$, then $C_{J \rightarrow I|K} = 0$.
- (b) (*No false positive*) If $N_I \subset K$, then $C_{J \rightarrow I|K} = 0$ for any set of nodes J .
- (c) (*True positive*) If $J \subset N_I$ and $J \not\subset K$, then $C_{J \rightarrow I|K} > 0$.
- (d) (*Decomposition*) $C_{J \rightarrow I|K} = C_{(K \cup J) \rightarrow I} - C_{K \rightarrow I}$.

Proof. Under the Temporal Markov Condition in Eq. (2.8), there is no time dependence of the distributions. For notational simplicity we denote the joint distribution $p(X_{t+1}^{(I)} = i, X_t^{(J)} = j, X_t^{(K)} = k)$ by $p(i, j, k)$ and use similar notation for the marginal and conditional distributions. It follows that

$$\begin{aligned}
 C_{J \rightarrow I|K} &= h(X_{t+1}^{(I)} | X_t^{(K)}) - h(X_{t+1}^{(I)} | X_t^{(K)}, X_t^{(J)}) = - \int p(i, j, k) \log \left[\frac{p(i|k)}{p(i|j, k)} \right] didj dk \\
 &\geq - \log \int p(i, j, k) \frac{p(i|k)}{p(i|j, k)} didj dk \quad (\text{by Jensen's inequality [?]}) \\
 (2.22) \quad &= - \log \int p(j, k) \frac{p(i, k)}{p(k)} didj dk = - \log(1) = 0,
 \end{aligned}$$

where equality holds if and only if $p(i|k) = p(i|j, k)$ *almost everywhere*. The above inequality is also known as the *Gibbs' inequality* in statistical physics [20].

To prove (a), we note that $J \subset K$ implies that $p(i|k) = p(i|j, k)$ and therefore equality holds (rather than inequality) in Eq. (2.22).

To prove (b), it suffices to show that for $J \not\subset K$, $C_{J \rightarrow I|K} = 0$. Since $J \not\subset K$ and $N_I \subset K$, based on the Spatial Markov Condition in Eq. (2.8), we have:

$$(2.23) \quad p(X_{t+1}^{(I)} | X_t) = p(X_{t+1}^{(I)} | X_t^{(K \cup J)}) = p(X_{t+1}^{(I)} | X_t^{(K)}) = p(X_{t+1}^{(I)} | X_t^{(N_I)}).$$

Therefore $p(i|j, k) = p(i|k)$ and equality holds in Eq. (2.22).

To prove (c), we use the Minimal Markov Condition in Eq. (2.8). Since $J \subset N_I$ and $J \not\subset K$, it follows that

$$(2.24) \quad p(X_{t+1}^{(I)} | X_t^{(K)}) = p(X_{t+1}^{(I)} | X_t^{(K \cap N_I)}) \neq p(X_{t+1}^{(I)} | X_t^{(K)}, X_t^{(J)}).$$

Thus, $p(i|j, k) \neq p(i|k)$ and strictly inequality holds in Eq. (2.22).

Finally, part (d) follows directly from the definition of C . \square

Theorem 2.2 allows us to convert the problem of causal network inference into the problem of estimating Causation Entropy among nodes. In particular, for a given set of nodes I , each node j can *in principle* be checked independently to determine whether or not it is a direct causal neighbor of I via either of the following two equivalent criteria (proved in Theorem 2.3(a) below)

$$(2.25) \quad \begin{cases} (1) \text{ Node } j \in N_I \text{ iff there is a set } K \supset N_I, \text{ such that } C_{j \rightarrow I|(K - \{j\})} > 0; \\ (2) \text{ Node } j \in N_I \text{ iff for any set } K \subset \mathcal{V}, C_{j \rightarrow I|(K - \{j\})} > 0. \end{cases}$$

Practical application of either criteria to infer large networks is challenging. Criterion (1) requires a conditioning set K that contains N_I as its subset. Since N_I is generally unknown, one often must use $K = \mathcal{V}$. When the network is large ($n \gg 1$), this requires the estimation of Causation Entropy for very high dimensional random variables from limited data, which is inherently unreliable [51, 52]. Criterion (2), on the other hand, requires a combinatorial search over all subsets making it computationally infeasible.

In the following we prove the two inference criteria in Eq. (2.25). Furthermore, we show that *the direct causal neighbor set is the minimal set of nodes that maximizes Causation Entropy*, which we refer to as the *Optimal Causation Entropy Principle*.

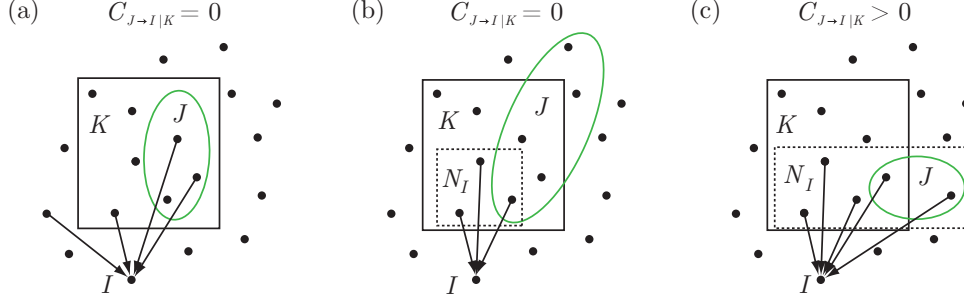


FIG. 2.2. Basic analytical properties of Causation Entropy (Theorem 2.2) allowing for the inference of the direct causal neighbors N_I of a set of nodes I . (a) Redundancy: If J is a subset of the conditioning set K ($J \subset K$), then the Causation Entropy $C_{J \rightarrow I|K} = 0$. (b) No false positive: If N_I is already included in the conditioning set K ($N_I \subset K$), then $C_{J \rightarrow I|K} = 0$. (c) True positive: If a set J contains at least one direct causal neighbor of I that does not belong to the conditioning set K , i.e., $(J \subset N_I) \wedge (J \not\subset K)$, then $C_{J \rightarrow I|K} > 0$.

THEOREM 2.3 (Optimal Causation Entropy Principle for Causal Network Inference). Suppose that the network stochastic process given by Eq. (2.4) satisfies the Markov properties in Eq. (2.8). Let $I \subset \mathcal{V}$ be a given set of nodes and N_I be the set of I 's direct causal neighbors, as defined in Eq. (2.3). It follows that

- (a) (Direct Inference) Node $j \in N_I$ iff $\Leftrightarrow \exists K \supset N_I$ such that $C_{j \rightarrow I|(K - \{j\})} > 0 \Leftrightarrow \forall K \subset \mathcal{V}, C_{j \rightarrow I|(K - \{j\})} > 0$.
- (b) (Partial Conditioning Removal) If there exists $K \subset \mathcal{V}$ such that $C_{j \rightarrow I|(K - \{j\})} = 0$, then $j \notin N_I$.
- (c) (Optimal Causation Entropy Principle) The set of direct causal neighbors is the minimal set of nodes with maximal Causation Entropy.

Define the family of sets with maximal Causation Entropy as

$$(2.26) \quad \mathcal{K} = \{K | \forall K' \subset \mathcal{V}, C_{K' \rightarrow I} \leq C_{K \rightarrow I}\}.$$

Then the set of direct causal neighbors satisfies

$$(2.27) \quad N_I = \cap_{K \in \mathcal{K}} K = \operatorname{argmin}_{K \in \mathcal{K}} K.$$

Proof. First we prove part (a). If $j \in N_I$, then for every $K \subset \mathcal{V}$, $C_{j \rightarrow I|(K - \{j\})} > 0$ following Theorem 2.2(c). This proves both " \Rightarrow ". On the other hand, suppose that $\forall K \subset \mathcal{V}, C_{j \rightarrow I|(K - \{j\})} > 0$, then for $K = \mathcal{V} \supset N_I$, it follows that $C_{j \rightarrow I|(\mathcal{V} - \{j\})} > 0$. Node $j \in N_I$ since otherwise $(\mathcal{V} - \{j\}) \supset N_I$ which would imply that $C_{j \rightarrow I|(\mathcal{V} - \{j\})} = 0$ from Theorem 2.2(b). Therefore, the two " \Leftarrow "s are also proven.

Next, part (b) follows directly from the contrapositive of Theorem 2.2(c).

Finally, we prove part (c). Note that if $N_I \not\subset K$, then $J = N_I - K \neq \emptyset$, and so $C_{(K \cup J) \rightarrow I} - C_{K \rightarrow I} = C_{J \rightarrow I|K} > 0$. Therefore, $K \in \mathcal{K} \Rightarrow N_I \subset K$. This implies $N_I \subset \cap_{K \in \mathcal{K}} K$. On the other hand, if $\exists j \in \cap_{K \in \mathcal{K}} K$ with $j \notin N_I$. Let $K \in \mathcal{K}$ and $L = K - \{j\}$. Since $j \notin N_I$, we have $N_I \subset L \subset K$, and therefore $C_{K \rightarrow I} - C_{L \rightarrow I} = C_{j \rightarrow I|L} = 0$, where the second equality follows from Theorem 2.2(c). This shows that $L \in \mathcal{K}$, contradicting with $j \in \cap_{K \in \mathcal{K}} K$. So $j \in \cap_{K \in \mathcal{K}} K \Rightarrow j \in N_I$, which implies that $\cap_{K \in \mathcal{K}} K \subset N_I$. Since \mathcal{K} is finite, it follows that $\cap_{K \in \mathcal{K}} K = \operatorname{argmin}_{K \in \mathcal{K}} K$. \square

Based on the Optimal Causation Entropy Principle, it seems straightforward to solve the minimax optimization for the inference of N_I by enumerating all subsets

of \mathcal{V} with increasing cardinality (starting from \emptyset), and terminating when a set K is found to be have maximal Causation Entropy among all subsets of cardinality $|K| + 1$ (i.e., adding any node j to set K does not increase the Causation Entropy $C_{K \rightarrow I}$). Based on Theorem 2.3, the set $K = N_I$. However, this brute-force approach requires $\mathcal{O}(n^{|N_I|})$ Causation Entropy evaluations, which is computationally inefficient and therefore infeasible for the inference of real world networks which often contain large number of nodes ($n \gg 1$). Such limitation is removed only when the number of direct causal neighbors is moderately small, $|N_I| = \mathcal{O}(1)$. In the following section we develop additional theory and algorithms to efficiently solve this minimax optimization problem for causal network inference.

2.5. Computational Causal Network Inference. Algorithmically, causal network inference via the Optimal Causation Entropy Principle should require as few computations as necessary (computational efficiency) and as few data samples as possible while retaining accuracy (data efficiency). We introduce two such algorithms that jointly infer the causal network. For a given node i , the goal is to infer its direct causal neighbors, as illustrated by nodes in the shaded region of Fig. 2.3(a). Algorithm 2.1 aggregatively identifies nodes that form a superset of the direct causal neighbors, $K \supset N_i$ (proven by Lemma 2.4, illustrated in Fig. 2.3(b)). Start from a set $K \supset N_i$, Algorithm 2.2 prunes away non-direct causal neighbors from K leaving only the direct causal neighbors N_i (proven by Lemma 2.5, illustrated in Fig. 2.3(c)).

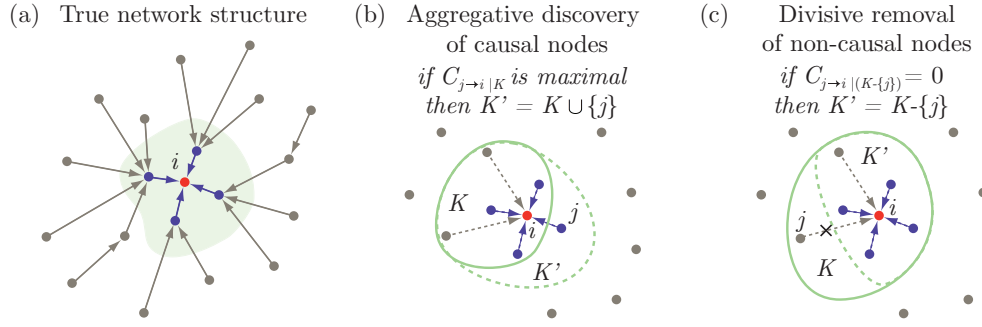


FIG. 2.3. Causal network inference by Optimal Causation Entropy. (a) Direct and indirect causal neighbors of a node i . Causal network inference corresponds to identifying the direct causal neighbors N_i (nodes in shaded region) for every node $i \in \mathcal{V}$. (b) Nodes are added to the set K in an aggregative fashion, maximizing Causation Entropy at each step (see Algorithm 2.1). (c) Starting from a set $K \supset N_i$ (K obtained by Algorithm 2.1), non-causal nodes are progressively removed from K if their Causation Entropy to node i conditioned on the rest of K is zero (see Algorithm 2.2).

LEMMA 2.4 (Aggregative Discovery of Causal Nodes). Suppose that the network stochastic process given by Eq. (2.4) satisfies the Markov properties in Eq. (2.8). Let $I \subset \mathcal{V}$ and N_I be its set of direct causal neighbors. Define the sequences of numbers $\{x_1, x_2, \dots\}$, nodes $\{p_1, p_2, \dots\}$, and nested sets $\{K_0, K_1, K_2, \dots\}$ as: $K_0 = \emptyset$, and

$$(2.28) \quad \begin{cases} x_i = \max_{x \in (\mathcal{V} - K_{i-1})} C_{x \rightarrow I | K_{i-1}}, \\ p_i = \operatorname{argmax}_{x \in (\mathcal{V} - K_{i-1})} C_{x \rightarrow I | K_{i-1}}, \\ K_i = \{p_1, p_2, \dots, p_i\} \end{cases}$$

for every $i \geq 1$. There exists a number q , with $|N_I| \leq q \leq n$, such that

(a) The numbers $x_i > 0$ for $1 \leq i \leq q$ and $x_i = 0$ for $i > q$.

(b) The set of direct causal neighbors $N_I \subset K_q = \{x_1, x_2, \dots, x_q\}$.

Proof. If $N_I = \emptyset$, the lemma holds trivially. Suppose that $|N_I| \geq 1$ and so $x_1 > 0$.

To prove (a), we define $q \equiv \min_{x_i=0}(i-1)$ (if all $x_i > 0$, define $q \equiv n$). By construction, $x_i > 0$ when $i \leq q$ and $x_{q+1} = 0$. This implies that $N_I \subset K_q$ since otherwise there is a node j with $C_{j \rightarrow I|K_q} > 0 \Rightarrow x_{q+1} > 0$. For any $i > q$, $N_I \subset K_q \subset K_{i-1}$, and thus $C_{j \rightarrow I|K_{i-1}} = 0$ for all $j \in (\mathcal{V} - K_{i-1})$, which implies that $x_i = 0$.

To prove (b), we note that if there is a node $j \in N_I$ such that $j \notin K_q$, then by the definition of x_i and Theorem 2.2(c), it follows that $x_{q+1} \geq C_{j \rightarrow I|K_q} > 0$. This is in contradiction with the fact that $x_i = 0$ for all $i > q$. Therefore, $N_I \subset K_q$. \square

Algorithm 2.1 recursively constructs the set $K_q \supset N_I$ (further denoted as K) as described by Lemma 2.4 and illustrated in Fig. 2.3(b). To remove indirect and spurious nodes in K that do not belong to N_I , we apply the result of Theorem 2.2(c), $C_{j \rightarrow I|(K-\{j\})} = 0 \Rightarrow j \notin N_I$. This gives rise to Lemma 2.5 and Algorithm 2.2.

LEMMA 2.5 (Progressive Removal of Non-Causal Nodes). *Suppose that the network stochastic process given by Eq. (2.4) satisfies the Markov properties in Eq. (2.8). Let $I \subset \mathcal{V}$ and N_I be its set of direct causal neighbors. Let $K = \{p_1, p_2, \dots, p_q\}$ such that $K \supset N_I$. Define the sequence of sets $\{K_0, K_1, K_2, \dots, K_q\}$ by $K_0 = K$, and*

$$(2.29) \quad K_i = \begin{cases} K_{i-1}, & \text{if } C_{p_i \rightarrow I|(K_{i-1}-\{p_i\})} > 0; \\ K_{i-1} - \{p_i\}, & \text{if } C_{p_i \rightarrow I|(K_{i-1}-\{p_i\})} = 0. \end{cases}$$

for every $1 \leq i \leq q$. Then $K_q = N_I$.

Proof. By definition, $K_0 = K \supset N_I$. We prove that $K_q \supset N_I$ by induction. Suppose that $K_{i-1} \supset N_I$. If node $p_i \in N_I$, then $C_{p_i \rightarrow I|(K_{i-1}-\{p_i\})} > 0$ by Theorem 2.2(c) and therefore $K_i = K_{i-1} \supset N_I$. If node $p_i \notin N_I$, then $K_i \supset K_{i-1} - \{p_i\} \supset N_I$.

Next we prove that $K_q \subset N_I$. Suppose that node $p_i \notin N_I$. Since $K_{i-1} \supset N_I$, the Causation Entropy $C_{p_i \rightarrow I|(K_{i-1}-\{p_i\})} = 0$ by Theorem 2.2(b), and so $K_i = K_{i-1} - \{p_i\}$. Therefore, $p \notin K_i \supset K_q$, which implies that $K_q \subset N_I$ (contrapositive). \square

Algorithm 2.2 iteratively removes non-direct causal neighbors from a set K until the set converges to N_I as described by Lemma 2.5 and illustrated in Fig. 2.3(c).

Jointly, Algorithms 2.1 and 2.2 can be applied to identify the direct causal neighbors of each node, thus inferring the entire causal network².

Algorithm 2.1 Aggregative Discovery of Causal Nodes

Input: Set of nodes $I \subset \mathcal{V}$

Output: K (which will include N_I as its subset)

- 1: Initialize: $K \leftarrow \emptyset$, $x \leftarrow \infty$, $p \leftarrow \emptyset$.
 - 2: **while** $x > 0$ **do**
 - 3: $K \leftarrow K \cup \{p\}$
 - 4: **for** every $j \in (\mathcal{V} - K)$ **do**
 - 5: $x_j \leftarrow C_{j \rightarrow I|K}$
 - 6: **end for**
 - 7: $x \leftarrow \max_{j \in (\mathcal{V} - K)} x_j$, $p \leftarrow \operatorname{argmax}_{j \in (\mathcal{V} - K)} x_j$
 - 8: **end while**
-

²Numerically estimated Causation Entropy is always positive due to finite sample size and numerical precision. In practice, one needs to use a statistical test (e.g., permutation test as described in Section 4) to examine the conditions $x > 0$ in Algorithm 2.1 and $C_{j \rightarrow I|(K-\{j\})} = 0$ in Algorithm 2.2.

Algorithm 2.2 Progressive Removal of Non-Causal Nodes

Input: Sets of nodes $I \subset \mathcal{V}$ and $K \subset \mathcal{V}$
Output: \hat{N}_I (inferred set of direct causal neighbors of I)

```

1: for every  $j \in K$  do
2:   if  $C_{j \rightarrow I|(K-\{j\})} = 0$  then
3:      $K \leftarrow K - \{j\}$ 
4:   end if
5: end for
6:  $\hat{N}_I \leftarrow K$ 

```

3. Application to Gaussian Process: Analytical Results. In this section we make analytical comparison among three approaches to causal network inference: Causation Entropy, Transfer Entropy [54], and Conditional Granger Causality [23, 24]. The next section will be devoted to the exploration of the numerical properties of these approaches for general random networks.

While information-theoretic approaches including Causation Entropy do not require stringent model assumptions, a linear model must be assumed to offer a fair comparison with the Conditional Granger Causality. As a benchmark example, we focus on the following linear discrete stochastic network dynamics

$$(3.1) \quad X_t^{(i)} = \sum_{j \in N_i} A_{ij} X_{t-1}^{(j)} + \xi_t^{(i)} \quad (\text{or in matrix form: } X_t = A X_{t-1} + \xi_t).$$

Here $X_t^{(i)} \in \mathbb{R}$ represents the state of node i at time t ($i \in \{1, 2, \dots, n\}, t \in \mathbb{N}$), $\xi_t^{(i)} \in \mathbb{R}$ represents noise, and $A_{ij} X_{t-1}^{(j)}$ models the influence of node j on node i . Equation (3.1) finds application in a broad range of areas, including time series analysis (as a multivariate linear autoregressive process [7]), information theory (as a network communication channel [12]), and nonlinear dynamical systems (as a linearized stochastic perturbation around equilibrium states [37]). It is straightforward to check that Eq. (3.1) is a special case of the general network stochastic process, Eq. (2.4), and asymptotically (as $t \rightarrow \infty$) satisfied the Markov assumptions in Eq. (2.8).

3.1. Analytical Properties of the Solution.

3.1.1. Solution Formula. Defining $X_0 = \xi_0$ for convenience, the solution to Eq. (3.1) can be expressed as

$$(3.2) \quad X_t = \sum_{k=0}^t A^k \xi_{t-k}.$$

We assume that $\xi_t^{(i)}$ are i.i.d Gaussian random variables with zero mean and finite nonzero variance, denoted as $\xi_t^{(i)} \sim N(0, \sigma_i^2)$ with $\sigma_i > 0$. Therefore,

$$(3.3) \quad \xi_t \sim N(0, S),$$

where the covariance matrix S is defined by $S_{ij} = \delta_{ij} \sigma_i^2$ with δ denoting the Kronecker delta. It follows that

$$(3.4) \quad \begin{cases} \mathbb{E}[\xi_t^{(i)}] = 0, \\ \text{Cov}(\xi_t^{(i)}, \xi_\tau^{(j)}) = \delta_{ij} \delta_{t\tau}. \end{cases}$$

Note that a random variable obtained by an affine transformation of a Gaussian variable is also Gaussian. For example, if $Y = [Y_1; Y_2]$ is Gaussian, the distribution of Y_1 conditioned on Y_2 is also Gaussian [16]. The proposition below follows by expressing random variables via appropriate affine transformations of ξ_t 's.

PROPOSITION 3.1. *Let I and K be any subsets of \mathcal{V} . Let $t \in \mathbb{N}$ and $\tau \in \{0\} \cup \mathbb{N}$. The conditional distribution of $X_{t+\tau}^{(I)}$ given $X_t^{(K)}$ is Gaussian.*

3.1.2. Covariance Matrix. Under an affine transformation from Gaussian variable Y to Z as $Z = CY + d$, the mean and covariance of Y and Z are related by: $\mu_Z = C\mu_Y + d$ and $\Sigma_Z = C\Sigma_Y C^\top$ [16]. We consider covariance matrices $\Phi(\tau, t)$, where the (i, j) -th entry of $\Phi(\tau, t)$ is defined as

$$(3.5) \quad \Phi(\tau, t)_{ij} \equiv \text{Cov}[x_{t+\tau}^{(i)}, x_t^{(j)}].$$

It follows from Eqs. (3.2) and (3.3) that

$$(3.6) \quad X_t \sim N(0, \Phi(0, t)), \text{ where } \Phi(0, t) = \sum_{k=0}^t A^k S (A^k)^\top.$$

In the following we prove a sufficient condition for the converge of the covariance matrix $\Phi(0, t)$ as time $t \rightarrow \infty$. Denote the *spectral radius* of a square matrix M by

$$(3.7) \quad \rho_M \equiv \max\{|\lambda| : \lambda \text{ is an eigenvalue of } M\}.$$

Note that $\rho_M = \rho_{M^\top}$ since a square matrix and its transpose have the same set of eigenvalues. For the dynamical system defined by Eq. (3.1), matrices A with $|\rho_A| < 1$ are the only matrices for which the underlying system poses a stable equilibrium in the absence of noise. We refer to these matrices as stable.

DEFINITION 3.2 (Stable Matrix). *Matrix M is stable if $\rho_M < 1$.*

The following is a known result from classical matrix theory [30].

THEOREM 3.3 (Convergence of Matrix Series [30]). *The matrix series $\sum_{k=0}^{\infty} M_k$ converges if the scalar series $\sum_{k=0}^{\infty} \|M_k\|$ under any induced norm $\|\cdot\|$ converges.*

Note that it is possible for the matrix series $\sum_{k=0}^{\infty} M_k$ to be convergent while the corresponding scalar series $\sum_{k=0}^{\infty} \|M_k\|$ diverges, analogous to the possibility of a scalar series that is convergent but not absolutely convergent. Next we state and prove a sufficient condition under which the matrix series in Eq. (3.6) converges.

PROPOSITION 3.4 (Convergence of the Covariance). *The series $\sum_{k=0}^{\infty} A^k S (A^k)^\top$ converges if A is stable.*

Proof. Let $\|\cdot\|$ be any induced norm. Then $\|A^k S (A^k)^\top\| \leq \|A^k\| \cdot \|S\| \cdot \|(A^\top)^k\|$ for any $k \in \mathbb{N}$. Gelfand's formula (see Ref. [19]) implies that

$$(3.8) \quad \lim_{k \rightarrow \infty} \|A^k\|^{1/k} = \lim_{k \rightarrow \infty} \|(A^\top)^k\|^{1/k} = \rho_A.$$

On the other hand, $\lim_{k \rightarrow \infty} \|S\|^{1/k} = 1$. Therefore,

$$\lim_{k \rightarrow \infty} \|A^k S (A^k)^\top\|^{1/k} \leq \lim_{k \rightarrow \infty} (\|A^k\| \cdot \|S\| \cdot \|(A^\top)^k\|)^{1/k} = \rho_A^2 < 1,$$

where the last inequality follows from the fact that A is stable. Hence the scalar series $\sum_{k=0}^{\infty} \|A^k S (A^k)^\top\|_2$ is convergent. The proposition follows by Theorem 3.3. \square

For the remainder of this section, it will be assumed that A is stable in Eq. (3.1). As $t \rightarrow \infty$, we drop the second argument in $\Phi(0, t)$ and define the *asymptotic covariance matrix*

$$(3.9) \quad \Phi(0) \equiv \lim_{t \rightarrow \infty} \Phi(0, t) = \sum_{k=0}^{\infty} A^k S (A^k)^\top.$$

It follows that $\Phi(0)$ satisfies an algebraic equation given by the proposition below.

PROPOSITION 3.5 (Asymptotic Covariance Matrix). *Assume that A is stable. The asymptotic covariance matrix $\Phi(0) = \sum_{k=0}^{\infty} A^k S (A^k)^\top$ satisfies the equation*

$$(3.10) \quad A\Phi(0)A^\top - \Phi(0) + S = 0.$$

Proof. Since A is stable, both of the two matrix series below converge:

$$\begin{cases} \Phi(0) = S + ASA^\top + A^2S(A^2)^\top + A^3S(A^3)^\top + \dots \\ A\Phi(0)A^\top = ASA^\top + A^2S(A^2)^\top + A^3S(A^3)^\top + \dots \end{cases}$$

Subtracting the two equations gives the result of the proposition. \square

Equation (3.10) is a (discrete) Lyapunov equation which often appears in stability analysis and optimal control problems [50]. Using “ \otimes ” as the Kronecker product and “vec” for the operation of transforming a square matrix to a column vector by stacking the columns of the underlying matrix in order, Eq. (3.10) can be converted into:

$$(3.11) \quad (I_{n^2} - A \otimes A) \text{vec}(\Phi(0)) = \text{vec}(S),$$

where I_{n^2} denotes the identity matrix of size n^2 -by- n^2 . Matrix $\Phi(0)$ can be computed by either solving Eq. (3.10) through iterative methods (see Ref. [3]) or by directly solving Eq. (3.11) as a linear system. In practice, we found the iterative approach to be numerically more efficient and stable compared to direct inversion.

Covariance matrices are in general positive semidefinite [16]. For the network dynamics defined in Eq. (3.1), we show that they are indeed positive definite.

PROPOSITION 3.6 (Positive Definiteness of the Covariance Matrix). *The covariance matrix $\Phi(0, t)$ is positive definite for any $t \in \mathbb{N}$. The asymptotic covariance matrix $\Phi(0)$ is also positive definite.*

Proof. For any unit vector $v \in \mathbb{R}^n$, $v^\top A\Phi(0, 0)A^\top v = (A^\top v)^\top A^\top v \geq 0$. From Eqs. (3.2) and (3.3), for any $t \in \mathbb{N}$, $\Phi(0, t) = A\Phi(0, t-1)A^\top + S$. By induction,

$$(3.12) \quad \begin{aligned} v^\top \Phi(0, t)v &= v^\top A\Phi(0, t-1)A^\top v + v^\top Sv \\ &\geq (A^\top v)^\top \Phi(0, t-1) (A^\top v) + \min_i \sigma_i^2 \geq \min_i \sigma_i^2 > 0. \end{aligned}$$

This shows that $\Phi(0, t)$ is positive definite (indeed we have: $\rho_{\Phi(0, t)} \geq \min_i \sigma_i^2 > 0$). Taking $t \rightarrow \infty$ in the above estimate also shows that $\Phi(0)$ is positive definite. \square

3.1.3. Time-Shifted Covariance Matrices. We define the time-shifted covariance matrix $\Phi(\tau, t)$ for each $t \in \mathbb{N}$ (time) and $\tau \in \mathbb{N}$ (positive time shift between states). If A is stable, then the covariance matrix $\Phi(t, \tau)$ converges for each time shift τ as $t \rightarrow \infty$. The (asymptotic) covariance matrices with different time shifts are related by a simple algebraic equation given in the following proposition.

PROPOSITION 3.7 (Relationship Between Time-Shifted Covariance Matrices). *Assume that A is stable. For each $\tau \in \mathbb{N}$, the following limit exists*

$$\lim_{t \rightarrow \infty} \Phi(\tau, t) = \Phi(\tau),$$

where matrix $\Phi(\tau)$ satisfies

$$(3.13) \quad \Phi(\tau) = A\Phi(\tau - 1) = A^2\Phi(\tau - 2) = \dots = A^\tau\Phi(0).$$

Proof. For every $\tau \in \mathbb{N}$ and $t \in \mathbb{N}$, it follows that

$$(3.14) \quad \Phi(\tau, t)_{ij} = \mathbb{E} \left[\sum_{k=1}^n a_{ik} x_{t+\tau-1}^{(k)} + \xi_{t+\tau}^{(i)}, x_t^{(j)} \right] = \sum_{k=1}^n a_{ik} \Phi(\tau - 1, t)_{kj}.$$

Therefore, the matrix $\Phi(\tau, t)$ satisfies

$$(3.15) \quad \Phi(\tau, t) = A\Phi(\tau - 1, t) = A^2\Phi(\tau - 2, t) = \dots = A^\tau\Phi(0, t).$$

Taking the limit as $t \rightarrow \infty$ in and making use of the fact that A is stable, we reach the conclusion of the proposition. \square

3.2. Analytical Expressions of Causation Entropy. Here we provide analytical expressions for Causation Entropy of the Gaussian process described in Eq. (3.1). Because Causation Entropy can be interpreted as a generalization of both Transfer Entropy and Conditional Granger Causality under the appropriate selection of nodes i and j and the conditioning set K , these results also provide analytical expressions for Transfer Entropy and Conditional Granger Causality.

3.2.1. Joint entropy expressions. Let Σ be the covariance matrix of a multivariate Gaussian variable $X \in \mathbb{R}^n$ (i.e., $X \sim N(\mu, \Sigma)$), it follows that [1]

$$(3.16) \quad h(X) = \frac{1}{2} \log[\det(\Sigma)] + \frac{1}{2} n \log(2\pi e).$$

Note that the right hand side of the above is actually an upper bound for a general random variable (i.e., the equality “=” becomes inequality “ \leq ” [12]). Therefore, a Gaussian variable maximizes entropy among all variables of equal covariance.

The random variable X_t is Gaussian and converges to $N(0, \Phi(0))$ as $t \rightarrow \infty$. For an arbitrary subset of the nodes $K = \{k_1, k_2, \dots, k_\ell\}$. The joint entropy is

$$(3.17) \quad h(X^{(K)}) = \lim_{t \rightarrow \infty} h(X_t^{(K)}) = \frac{1}{2} \log(|\Phi_{KK}(0)|) + \log(2\pi e).$$

Here we have introduced the notation

$$(3.18) \quad \Phi_{IJ}(0) \equiv P(I)\Phi(0)P(J)^\top,$$

where for a set $K = \{k_1, k_2, \dots, k_\ell\}$, $P(K)$ is the ℓ -by- n projection matrix defined as

$$(3.19) \quad P(K)_{ij} = \delta_{k_i, i}$$

3.2.2. Causation Entropy. For the Gaussian process given by Eq. (3.1), we obtain the analytical expression of Causation Entropy as

$$(3.20) \quad C_{J \rightarrow I|K} = \frac{1}{2} \log \left(\frac{\det [\Phi(0)_{II} - \Phi(1)_{IK} \Phi(0)_{KK}^{-1} \Phi(1)_{IK}^\top]}{\det [\Phi(0)_{II} - \Phi(1)_{I, K \cup J} \Phi(0)_{K \cup J, K \cup J}^{-1} \Phi(1)_{I, K \cup J}^\top]} \right)$$

If $J = \{j\}$ and $I = \{i\}$, this equation simplifies to

$$(3.21) \quad C_{j \rightarrow i|K} = \frac{1}{2} \log \left(\frac{\Phi(0)_{ii} - \Phi(1)_{iK} \Phi(0)_{KK}^{-1} \Phi(1)_{iK}^\top}{\Phi(0)_{ii} - \Phi(1)_{i, K \cup \{j\}} \Phi(0)_{K \cup \{j\}, K \cup \{j\}}^{-1} \Phi(1)_{i, K \cup \{j\}}^\top} \right).$$

3.2.3. Transfer Entropy. Recall that Causation Entropy recovers Transfer Entropy when $K = \{i\}$. Letting $K = \{i\}$ in the formula above gives the Transfer Entropy (with single time lag) for multivariate Gaussian variables:

$$(3.22) \quad T_{j \rightarrow i} = C_{j \rightarrow i|i} = \frac{1}{2} \log \left(1 + \frac{\alpha_{ij}}{\beta_{ij} - \alpha_{ij}} \right),$$

where $\begin{cases} \alpha_{ij} \equiv (\Phi(0)_{ii}\Phi(1)_{ij} - \Phi(0)_{ij}\Phi(1)_{ii})^2, \\ \beta_{ij} \equiv (\Phi(0)_{ii}^2 - \Phi(1)_{ii}^2)(\Phi(0)_{ii}\Phi(0)_{jj} - \Phi(0)_{ij}^2). \end{cases}$

It follows that $\beta_{ij} \geq \alpha_{ij} \geq 0$, and therefore $T_{j \rightarrow i} \geq 0$ ($T_{i \rightarrow i} = 0$). Furthermore,

$$(3.23) \quad T_{j \rightarrow i} = 0 \iff \alpha_{ij} = 0 \iff \sum_{k=1}^n A_{ik} (\Phi(0)_{ii}\Phi(0)_{kj} - \Phi(0)_{ij}\Phi(0)_{ki}) = 0.$$

3.2.4. Conditional Granger Causality. As shown in Ref. [2], when the random variables are Gaussian, expression of Granger Causality is equivalent as that of Transfer Entropy (and also Causation Entropy introduced here). In fact, for Gaussian variables, the Granger Causality from j to i without conditioning equals $2C_{j \rightarrow i}$, while the Conditional Granger Causality (with full conditioning) equals $2C_{j \rightarrow i|(V - \{j\})}$.

3.3. Analytical Results for Directed Linear Chain, Directed Loop, and Directed Trees. We derive expressions of Transfer Entropy and Causation Entropy for several classes of networks including directed linear chains, directed loops, and directed trees. These results highlight that although Transfer Entropy may indicate the direction of information flow between two nodes, its application to causal network inference is often unjustified as it cannot distinguish between direct and indirect causal relationships (unless appropriate conditioning is adopted as in Causation Entropy).

3.3.1. Directed Linear Chain. Denote a directed linear chain of n nodes as

$$(3.24) \quad 1 \rightarrow 2 \rightarrow 3 \cdots \rightarrow n.$$

For simplicity we assume that all links have the same weight $w = 1$. Consequently, the corresponding adjacency matrix $A = [A_{ij}]_{n \times n}$ is given by

$$(3.25) \quad A_{ij} = \delta_{i,j+1}.$$

It follows that $\rho_A = 0$ and therefore A is stable. By inverting the lower-triangular matrix $(I_{n^2} - A \otimes A)$ in Eq. (3.11) and applying Eq. (3.13), we obtain that

$$(3.26) \quad \begin{cases} \Phi(0)_{ij} = \delta_{ij} \sum_{k=1}^j \sigma_k^2, \\ \Phi(1)_{ij} = \delta_{i,j+1} \sum_{k=1}^j \sigma_k^2. \end{cases}$$

Letting $K = \emptyset$ and $K = \{i\}$ respectively in Eqs. (3.21) and (3.22), it follows that

$$(3.27) \quad C_{j \rightarrow i} = T_{j \rightarrow i} = \frac{1}{2} \delta_{i,j+1} \log \left(1 + \frac{\sum_{k=1}^j \sigma_k^2}{\sigma_i^2} \right).$$

Therefore, for the directed linear chain defined in Eq. (3.25), Transfer Entropy $T_{j \rightarrow i} = C_{j \rightarrow i}$, and it is positive if and only if there is a direct link $j \rightarrow i$, i.e.,

$$(3.28) \quad C_{j \rightarrow i} = T_{j \rightarrow i} > 0 \iff A_{ij} = 1, \text{ and } C_{j \rightarrow i} = T_{j \rightarrow i} = 0 \iff A_{ij} = 0.$$

Interestingly, both Causation Entropy $C_{j \rightarrow j+1}$ and Transfer Entropy $T_{j \rightarrow j+1}$ increase monotonically as a function of j , and the values only depend on part of the chain from the top node (node 1) to node $j+1$ and not on the rest of the network. Interpreting the monotonicity in term of the network structure, the closer node j is to the end of the chain, effectively the more information is transferred through the directed link $j \rightarrow j+1$. Figure. 3.1(a) illustrates this via a network of $n = 1000$ nodes.

3.3.2. Directed Loop. Consider now a directed loop with n nodes, denoted as

$$(3.29) \quad 1 \rightarrow 2 \rightarrow 3 \cdots \rightarrow n \rightarrow 1.$$

Let $w > 0$ be the uniform link weight. It follows that $\rho_A = w$. Thus, for the adjacency matrix A to be stable, we must have $w < 1$. To keep the symmetry of the problem, we further assume that the variance of noise is the same at each node, therefore

$$(3.30) \quad \sigma^2 \equiv \sigma_1^2 = \sigma_2^2 = \dots \sigma_n^2.$$

The entries in $\Phi(0, t)$ satisfy

$$(3.31) \quad \Phi(0, t)_{ij} = w^2 \Phi(0, t-1)_{p_i, p_j} + \delta_{ij} \sigma^2,$$

where p_i denotes the unique node that directly links to node i . Taking the limit as $t \rightarrow \infty$ and solve the resulting recursive equations, we obtain that for

$$(3.32) \quad \begin{cases} \Phi(0)_{ij} = \delta_{ij} \sigma^2 / (1 - w^2), \\ \Phi(1)_{ij} = \delta_{p_i, j} \sigma^2 w / (1 - w^2). \end{cases}$$

where the second equation is obtained through $\Phi(0)_{ij}$ and Eq. (3.13). Letting $K = \emptyset$ and $K = \{i\}$ respectively in Eqs. (3.21) and (3.22), we conclude that

$$(3.33) \quad C_{j \rightarrow i} = T_{j \rightarrow i} = \frac{1}{2} \delta_{p_i, j} \log \left(\frac{1}{1 - w^2} \right).$$

Note that Causation Entropy and Transfer Entropy equal and do not depend on the noise variation σ^2 , and they are positive if and only if there is a direct link $j \rightarrow i$, i.e.,

$$(3.34) \quad C_{j \rightarrow i} = T_{j \rightarrow i} > 0 \Leftrightarrow A_{ij} = 1, \text{ and } C_{j \rightarrow i} = T_{j \rightarrow i} = 0 \Leftrightarrow A_{ij} = 0.$$

By symmetry, Causation Entropy and Transfer Entropy through each directed link is the same. As the link weight w increases in $(0, 1)$, both increase monotonically in $(0, \infty)$. The larger the link weight w is, the larger amount of information is transferred via each directed link, as intuitively expected. Also see Fig. 3.1(b) as an illustration.

3.3.3. Directed Trees. We now consider directed tree networks with uniform link weight $w = 1$ and unit node variance³

$$(3.35) \quad \sigma_1^2 = \sigma_2^2 = \dots \sigma_n^2 = 1.$$

A directed tree has one root (indexed as node 1 without loss of generality) and each non-root node i ($i \neq 1$) has exactly one *ancestor*, denoted by p_i . The corresponding adjacency matrix $A = [A_{ij}]_{n \times n}$ thus satisfies

$$(3.36) \quad A_{ij} = (1 - \delta_{i1}) \delta_{i, p_i}.$$

³Similar results hold for trees with general link weights and node variances but the corresponding equations are too cumbersome to list.

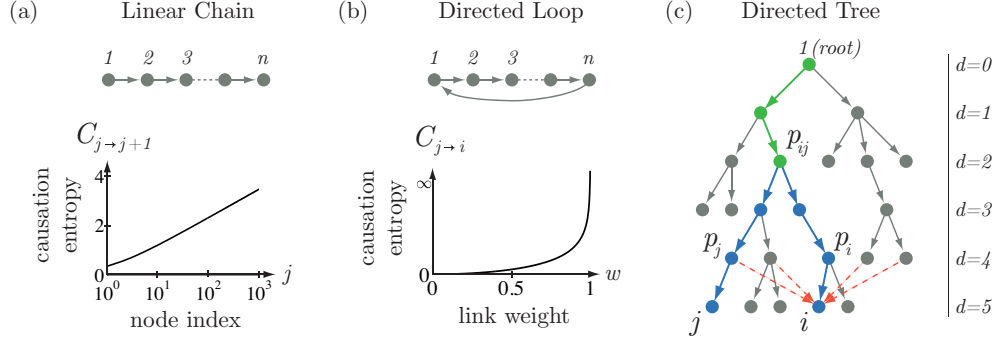


FIG. 3.1. *Causation Entropy and Transfer Entropy for a Gaussian process on three classes of networks.* (a) For directed linear chains, both Causation Entropy and Transfer Entropy correctly identify the network as $C_{j \rightarrow i} = T_{j \rightarrow i} > 0$ iff $i = j+1$ (otherwise $C_{j \rightarrow i} = T_{j \rightarrow i} = 0$). The dependence of $C_{j \rightarrow j+1}$ on node index j is given by Eq. (3.27) and plotted. (b) For directed loops, Causation Entropy and Transfer Entropy again correctly identify the network topology with $C_{j \rightarrow i} = T_{j \rightarrow i} > 0$ iff $j \rightarrow i$. The dependence of $C_{j \rightarrow i}$ on link weight w is given by Eq. (3.33) as shown. (c) For directed trees, Causation Entropy given by Eq. (3.41) correctly identifies the network topology based on Eq. (3.43). In contrast, Transfer Entropy without appropriate conditioning infers many links that do not exist in the actual network (red dashed lines), as described by Eq. (3.42).

It can be shown that $\rho_A = 0$. For $i \neq 1$, we denote the directed path from 1 to i by

$$(3.37) \quad 1 = p_i^{(d_i)} \rightarrow p_i^{(d_i-1)} \rightarrow \dots \rightarrow p_i^{(1)} \equiv p_i \rightarrow p_i^{(0)} \equiv i,$$

where d_i is the *depth* of node i in the tree (for node 1, we define its depth $d_1 = 0$). Thus, the highest node in the tree is the root, and the lowest nodes have the greatest depth. For any two nodes (i, j) , we denote their *lowest common ancestor* by p_{ij} , i.e.,

$$(3.38) \quad p_{ij} = \arg \max_{\{k | \exists \ell, m \geq 0, s.t., p_i^{(\ell)} = p_j^{(m)}\}} d_k.$$

The covariance matrix $\Phi(0, t)$ satisfies

$$(3.39) \quad \Phi(0)_{ij} = \delta_{1i} \delta_{1j} \sigma_1^2 + (1 - \delta_{1i})(1 - \delta_{1j})[\Phi(0)_{p_i, p_j} + \delta_{ij}].$$

We solve these recursive equations to obtain

$$(3.40) \quad \begin{cases} \Phi(0)_{ij} = \delta_{d_i, d_j} (d_{p_{ij}} + 1) \\ \Phi(1)_{ij} = (1 - \delta_{i1}) \delta_{d_i, d_j+1} (d_{p_{ij}} + 1), \end{cases}$$

where p_{ij} is defined in Eq. (3.38) and $\Phi(1)_{ij}$ is obtained by $\Phi(1) = A\Phi(0)$.

We calculate Causation Entropy and Transfer Entropy through Eqs. (3.21) and (3.22):

$$(3.41) \quad C_{j \rightarrow i} = T_{j \rightarrow i} = \frac{1}{2} \delta_{d_i, d_j+1} \log \frac{(d_i + 1)(d_j + 1)}{(d_i + 1)(d_j + 1) - (d_{p_{ij}} + 1)^2}.$$

Note that in general $0 \leq d_{p_{ij}} \leq \min\{d_i, d_j\}$. Thus $C_{j \rightarrow i} = T_{j \rightarrow i} \leq \frac{1}{2} \log(1 + d_i)$, with equality if and only if j is the ancestor of i (i.e., $j = p_i = p_{ij}$). Therefore, we have

$$(3.42) \quad \begin{cases} T_{j \rightarrow i} > 0 \Leftrightarrow d_i = d_j + 1 \Leftarrow A_{ij} = 1 \text{ (but } T_{j \rightarrow i} > 0 \not\Leftrightarrow A_{ij} = 1); \\ T_{j \rightarrow i} = 0 \Leftrightarrow d_i \neq d_j + 1 \Rightarrow A_{ij} = 0 \text{ (but } A_{ij} = 0 \not\Leftrightarrow T_{j \rightarrow i} = 0). \end{cases}$$

In other words, Transfer Entropy being positive (without appropriate conditioning) corresponds to a superset of the links that actual exist in a directed tree, and the inferred network using this criterion will potentially contain many false positives. See Fig. 3.1(c) as an example. On the other hand, for a given node $i \neq 1$, we have

$$(3.43) \quad \begin{cases} p_i = \arg \max_j C_{j \rightarrow i}, \\ C_{j \rightarrow i | \{p_i\}} = 0. \end{cases}$$

Therefore, for each node i , the node j that maximizes Causation Entropy $C_{j \rightarrow i}$ among all nodes is inferred as the direct causal neighbor of i . Conditioned on this node, the Causation Entropy from any other node to i will become zero, indicating no other directed links to node i . This Causation Entropy based procedure allows for exact and correct inference of the underlying causal network, a directed tree.

4. Application to Gaussian Process: Numerical Results. In this section, we illustrate that causal network inference by Optimal Causation Entropy is reliable and efficient for the Gaussian process, Eq. (3.1), on large random networks.

4.1. Random Network Model and Time Series Generation. We consider signed Erdős-Rényi networks, which is a generation of its original model [5]. In particular, each network consists of n nodes ($\mathcal{V} = \{1, 2, \dots, n\}$), such that each directed link $j \rightarrow i$ is formed independently with equal probability p , giving rise to a directed network with approximately $n^2 p$ directed links. For generality, we allow the link weight of each link $j \rightarrow i$ to be either positive ($e_{ij} = w$) or negative ($e_{ij} = -w$), with equal probability. Recalling that the network adjacency matrix A is defined entry-wise by $A_{ij} = e_{ij} \in \{w, -w\}$ iff there exists a directed link $j \rightarrow i$ (otherwise $A_{ij} = 0$), the link weight w may be selected to tune the spectral radius $\rho(A)$ of matrix A .

We generate time series from the stochastic equation, Eq. (3.1), where matrix A is obtained from the network model and random variables $\xi_t \sim \mathcal{N}(0, S)$, where the covariance matrix S is taken to be the identity matrix of size $n \times n$. To reduce transient effects, for a given sample size T we solve Eq. (3.1) for $10T$ time steps and only use the final 10% of the resulting time series.

To summarize, our numerical experiments contain parameters: n (network size), p (connection probability), $\rho(A)$ (spectral radius of A), and T (sample size).

4.2. Practical Considerations for Network Inference. We have established by Theorems 2.2 and 2.3 and Lemmas 2.4 and 2.5 that in theory, exact network inference can be achieved by Optimal Causation Entropy, which involves implementing Algorithms 2.1 (Aggregative Discovery) and 2.2 (Progressive Removal) to correctly identify the set of direct causal neighbors N_i for each node $i \in \mathcal{V}$.

In practice, the success of our Optimal Causation Entropy approach (and in fact, any entropy-based approaches) depends crucially on reliable estimation of the relevant entropies in question from data. This leads to two practical challenges.

(1) Entropies must be *estimated* from *finite* time series data. While there are several techniques for estimating entropies for general multivariate data, the accuracy of such estimations are increasingly inaccurate for small sample sizes and high-dimensional random variables [45]. In this research, we side-step this computational complexity by using knowledge of the asymptotic functional form for the entropy of the Gaussian Process, where the covariance matrices $\Phi(0)$ and $\Phi(1)$ in Eqs. (3.20) and (3.21) are estimated directly from the time series data.

(2) Application of the theoretical results rely on determining whether the Causation Entropy $C_{j \rightarrow i | K} > 0$ or $C_{j \rightarrow i | K} = 0$. However, the estimated value of $C_{j \rightarrow i | K}$

based on sample covariances is necessarily positive given finite sample size and finite numerical precision. Therefore, a statistical test must be used to assess the significance of the observed positive Causation Entropy. We here adopt a widely used approach in non-parametric statistics, called the *permutation test*⁴. Specifically, we propose the following permutation test based on the null hypothesis that Causation Entropy $C_{j \rightarrow i|K} = 0$: first perform r random (temporal) permutations of the time series $\{X_t^{(j)}\}$, leaving the rest of the data unchanged; we then construct an empirical cumulative distribution $\hat{F}(x)$ of the estimated Causation Entropy from the permuted time series⁵; finally, given a prescribed significance level θ , the observed $C_{j \rightarrow i|K} = c$ is declared *significant* (i.e., the null hypothesis is rejected at level θ) if $\hat{F}(c) > \theta$.

To summarize, the inference algorithms contain two parameters to be used in the permutation test: r (number of random permutations) and θ (significance threshold).

4.3. Comparing Optimal Causation Entropy, Conditional Granger, and Transfer Entropy. Here we compare the performance of three approaches of causal network inference: Conditional Granger (see for example Ref. [18, 26]), Transfer Entropy (see Ref. [65] and the references therein), and Optimal Causation Entropy (Optimal CSE). In particular, the Conditional Granger and Transfer Entropy approaches under consideration both estimate the entropy $C_{j \rightarrow i|K}$ for each pair of nodes (i, j) independently, with the choice of $K = \mathcal{V} - \{j\}$ in the case of Conditional Granger and $K = \{i\}$ in the case of Transfer Entropy. In both approaches, a causal link $j \rightarrow i$ is inferred if the observed $C_{j \rightarrow i|K} > 0$ is assessed as significant under the permutation test. The Optimal CSE approach combines Algorithms 2.1 and 2.2 and the permutation test is used once per each iteration (line 2 of both algorithms).

The performance of the three approaches are quantified by two types of inference error: false negative ratio, denoted as ε_- and defined as the fraction of links in the original network that are not inferred; and false positive ratio, denoted as ε_+ and defined as the fraction of non-existing links in the original networks that are inferred. In terms of the adjacency matrix A of the original network and that of the inferred network \hat{A} , these ratios can be computed as

$$(4.1) \quad \begin{cases} \varepsilon_- \equiv \frac{\text{number of } (i, j) \text{ pairs with } \chi_0(A)_{ij} = 1 \text{ and } \chi_0(\hat{A})_{ij} = 0}{\text{number of } (i, j) \text{ pairs with } \chi_0(A)_{ij} = 1}, \\ \varepsilon_+ \equiv \frac{\text{number of } (i, j) \text{ pairs with } \chi_0(A)_{ij} = 0 \text{ and } \chi_0(\hat{A})_{ij} = 1}{\text{number of } (i, j) \text{ pairs with } \chi_0(A)_{ij} = 0}. \end{cases}$$

For the random networks considered here, we found that the Algorithm 2.1 achieves almost the same accuracy as the combination of Algorithms 2.1 and 2.2. We therefore present results which are based on the numerical application of Algorithm 2.1 alone, leaving detailed numerical study of Algorithm 2.2 to future work.

Figure 4.1(a-b) shows that although the Conditional Granger approach is theoretically correct and works well for small network size with sufficient samples, it suffers from increasing inference error as the network size increases and become extremely

⁴The idea of a permutation test is to perform (large number of) random permutations of a subset of the data leaving the rest unchanged, giving rise to an empirical distribution of the static of interest. The observed statistic from the original data is then located on this empirical distribution in order to associate its statistical significance [22].

⁵The accuracy of this empirical distribution and therefore the permutation test increases with increasing number of permutations r . However, as r increases, the computational complexity also increases, scaling roughly as a linear function of r .

inaccurate when the network size n starts to surpass the sample size T . Such limitation is overcome by the Optimal CSE approach, where both the false positive and false negative ratios remain close to zero as the network size increases. The reason that Optimal CSE is accurate even as n increases is that it builds the causal neighbor set in an *aggregative* manner, therefore relying only on estimating entropy in relatively low dimensions (roughly the same dimension as the number of neighbors per node). In sharp contrast, the Conditional Granger approach requires the estimation of entropy in the full n -dimensional space and therefore requires many (potentially exponentially) more samples to achieve the same accuracy when n becomes large.

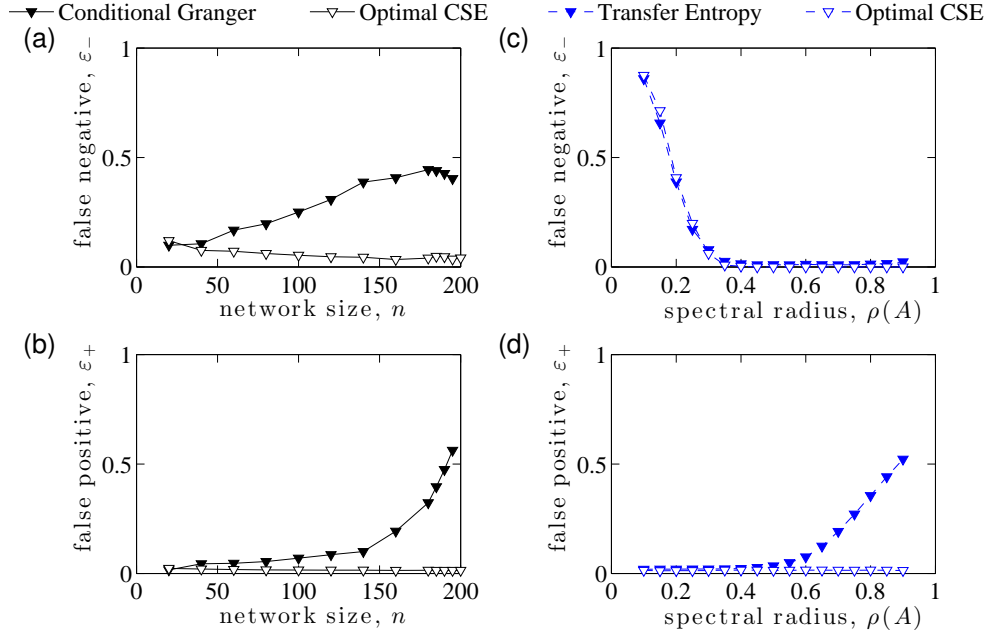


FIG. 4.1. Comparison of causal network inference approaches: Conditional Granger, Transfer Entropy, and Optimal CSE. The time series are generated from the Gaussian process defined in Eq. (3.1) using signed Erdős-Rényi networks (see Sec 4.2 for details). Two types of inference error are examined: false negative and false positive ratios, defined in Eq. (4.1). (a-b) Inference error as a function of network size n using Conditional Granger versus Optimal CSE approaches. Here the networks have fixed average degree $np = 10$ and spectral radius $\rho(A) = 0.8$. Sample size is $T = 200$. (c-d) Inference error as a function of the spectral radius $\rho(A)$ using Transfer Entropy versus Optimal CSE approaches. Here the networks have fixed number of nodes $n = 200$ and average degree $np = 10$. Sample size is $T = 2000$. For all three approaches we apply the permutation test using $r = 100$ permutations and significance level $\theta = 99\%$. Each data point is obtained from averaging over 20 independent simulations of the network dynamics, Eq. (3.1).

Figure 4.1(c-d) shows that even for a sufficient number of samples, the Transfer Entropy approach without appropriate conditioning can lead to considerable inference error, and is therefore inherently unsound for causal network inference. In particular, although inference by both Transfer Entropy and Optimal CSE give similar false negatives in the regime of $\rho(A) \approx 0$ where the dynamics is dominated by noise and not the causal dependences, Transfer Entropy yields increasing false positives when the causal links dominate, $\rho(A) \rightarrow 1$. This is mainly due to the fact that as $\rho(A) \rightarrow 1$, indirect causal nodes become increasingly difficult to distinguish from direct ones without appropriate conditioning [61]. Optimal CSE, on the other hand, consistently

yields nearly zero false positive ratios in the entire range of $\rho(A)$. Interestingly, the spectral radius $\rho(A)$ can be interpreted as the *information diffusion rate* on networks and found to be very close to criticality (i.e., $\rho(A) \approx 1$) in neuronal networks [33, 36].

These numerical experiments highlight that whereas the Conditional Granger approach is inaccurate for $T \lesssim n$ and the Transfer Entropy approach is inaccurate when $\rho(A) \lesssim 1$, the proposed Optimal CSE approach overcomes both limitations and yields almost exact network inference even for limited sample size.

4.4. Performance of Optimal Causation Entropy Approach for Causal Network Inference. Having established the advantages of the Optimal CSE approach, we now examine its performance under various parameter settings.

First, we examine the effect of the significance level θ on the inference error. As shown in Fig. 4.2(a-b), the false negative ratio ϵ_- does not seem to depend on θ and converges to zero as sample size T increases. On the other hand, as $T \rightarrow \infty$, the false positive ratio saturates at the level $\epsilon_+ \sim (1 - \theta)$, which is consistent with the implementation of the permutation test which rejects the null hypothesis at θ . This observation suggests that in order to achieve higher accuracy given sufficient sample size, one should choose θ as close to one as possible. The tradeoff in practice is that reliable implementation using larger θ requires an increasing number of permutations and therefore increases the computational complexity of the inference algorithms.

Next, we investigate the effect of sample size T on the inference error for networks of different sizes. The results are shown in Fig. 4.2(c-d). As expected, when T increases, the false negative ratio decreases towards zero. Somewhat unexpectedly, the false positive ratio stays close to zero (in fact, close to the significance level θ) even for relatively small sample size (T as small as 50 for networks of up to 500 nodes). Furthermore, it appears that for networks of different sizes but the same average degree and information diffusion rate, the false negative ratios drop close to zero almost at the same sample size. To better quantify these effects, we define the *critical sample size* T_* as the smallest number of samples for which the false negative ratio falls below $1 - \theta$. As shown in the inset of Fig. 4.2(c), for networks with the same average degree and information diffusion rate, the critical sample size T_* remains mostly constant despite the increase of the network size. This result is unexpected. Traditionally, the network size n represents a lower bound on sample size T as any covariance matrix (e.g., application of the Conditional Granger requires that $T > n$ for the invertibility of the covariance matrices). Our result surprisingly indicates that sample size T does not need to scale with network size n for accurate network inference, and highlights the fact that the Optimal CSE approach is *scalable* and *data efficient*, with accuracy depending *not* on the size of the network, but rather on other network characteristics such as the density of links and spectral radius.

To strengthen our claim that for Erdős-Rényi networks, performance of the causal inference by the Optimal CSE approach depends on the density of links as measured by average degree and information diffusion rate as measured by the spectral radius rather than network size, we further investigate the dependence of inference error on these two additional parameters, np and $\rho(A)$. As shown in Fig. 4.3(a), for networks of the same size $n = 200$ with fixed $\rho(A) = 0.8$, the larger the average degree np , the larger the number of samples required to reduce the false negative ratio to zero. In fact, as shown in the inset of Fig. 4.3(a), the critical sample T_* to reach $\epsilon_- < 1 - \theta$ appears to scale *linearly* as a function of the average degree np , but not the network size (see the inset of Fig. 4.2(c)). On the other hand, Fig. 4.3(c-d) shows that the information diffusion rate, $\rho(A)$, seems to pose a harder constraint on accurate

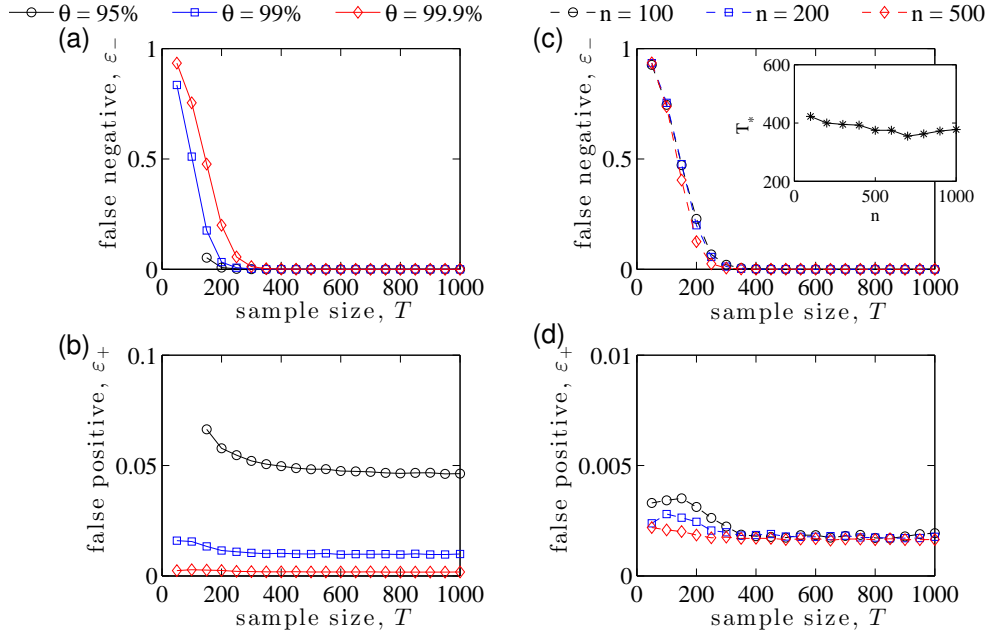


FIG. 4.2. Performance of the Optimal CSE approach for causal network inference with different significance threshold for networks of various sizes. The time series are generated from the Gaussian process defined in Eq. (3.1) using signed Erdős-Rényi networks (see Sec 4.2 for details). False negative ratio (upper row) and false positive ratio (lower row) are defined in Eq. (4.1). (a-b) Inference error as a function of sample size T for various significance levels θ used in the permutation test. Here networks have $n = 200$ nodes with expected average degree $np = 10$ and information diffusion rate $\rho(A) = 0.8$. (c-d) Inference error as a function of sample size T for various network sizes. Here networks have the same expected average degree $np = 10$ and information diffusion rate $\rho(A) = 0.8$, and we use $r = 1000$ permutations in the permutation test with $\theta = 0.999$. Note that all three false negative curves in (c) appear to converge for $T \approx 300$. The critical sample size T_* (defined as the minimum T for which $\epsilon_- < 1 - \theta$) as a function of the network size n is shown in the inset of (c), suggesting the absence of scaling of T_* in terms of n . Each data point is obtained from averaging over 20 independent simulations of the network dynamics, Eq. (3.1).

network inference: the smaller it is, the more samples that are needed for accuracy. In particular, as shown in the inset of Fig. 4.3(c), the critical sample size appears to increase *exponentially* as $\rho(A)$ decreases towards zero. Interestingly, as shown in Fig. 4.3(b,d), the false positive ratios in both cases remain close to its saturation level around $1 - \theta = 10^{-3}$ even for very small sample size ($T \sim 50$), and this holds across networks with different average degree and different size (also see Fig. 4.2(d)).

To briefly summarize these numerical experiments, we found that for the Gaussian process, practical causal network inference by the proposed Optimal CSE overcomes fundamental limitations of previous approaches including Conditional Granger and Transfer Entropy. One important advantage of the Optimal CSE approach as suggested by the numerical results is that it often requires a relatively small number of samples to achieve high accuracy, making it a data-efficient method to use in practice. In fact, we found that for Erdős-Rényi networks, the critical number of samples required for the false negatives to vanish does not depend on the network size, but rather depends on the density of links (as measured by average degree) and the information diffusion rate (as measured by the spectral radius of the network adjacency

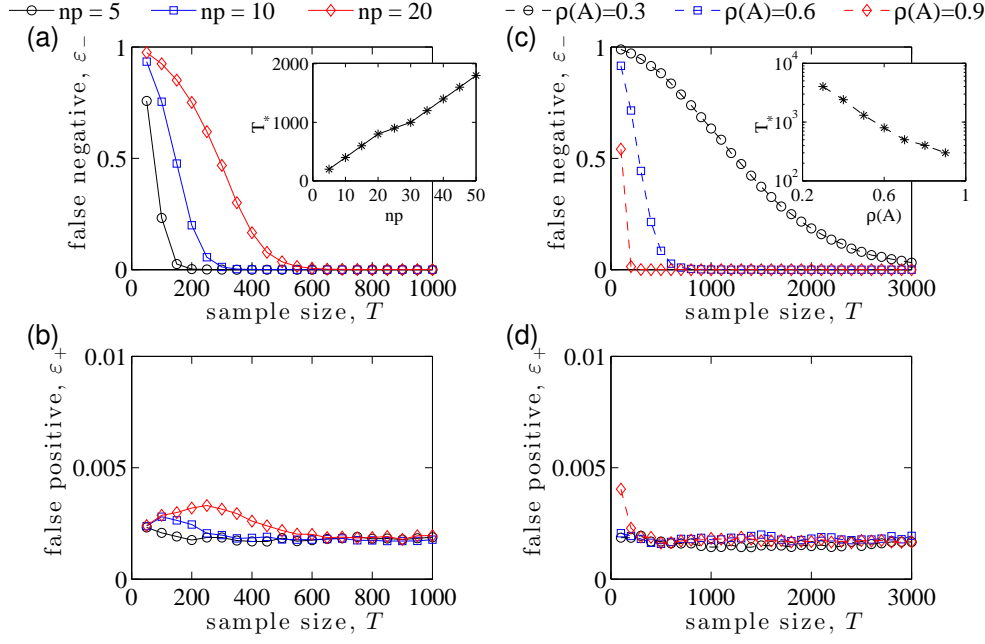


FIG. 4.3. Performance of the Optimal CSE approach for causal network inference for networks with different average degree and spectral radius. The time series are generated from the Gaussian process defined in Eq. (3.1) using signed Erdős-Rényi networks (see Sec 4.2 for details). False negative ratio (upper row) and false positive ratio (lower row) are defined in Eq. (4.1). (a-b) Inference error as a function of sample size for networks with various average degree np . Here the networks have the same size $n = 200$ and spectral radius $\rho(A) = 0.8$. The inset shows the critical sample size T_* (see text) as a function of np . (c-d) Inference error as a function of sample size for networks with various spectral radii $\rho(A)$. Here the networks have the same size $n = 200$ and average degree $np = 10$. The permutation test used for the data in all panels involve $r = 1000$ permutations with the significance threshold $\theta = 0.999$. Each data point is obtained from averaging over 20 independent simulations of the network dynamics, Eq. (3.1).

matrix). This is somewhat surprising because traditionally the network size poses as an absolute lower bound for the sample size in order for proper inversion of the covariance matrix (recent advances such as *Lasso* has partially resolved this issue by making specific assumptions of the model form and utilizing l_1 optimization techniques [17, 63]). On the other hand, our numerical results also suggest that only a very small number of samples is needed for the false positives to reach its saturation level. This level is inherently set by the significance threshold used in the permutation test rather than other network characteristics and can be systematically reduced by increasing the significance threshold and the number of permutations.

5. Discussion and Conclusion. Although time series analysis is broadly utilized for scientific research, the inference of large networks from relatively short times series data, and in particular causal networks describing “cause-and-effect” relationships, has largely remained unresolved. The main contribution of this paper includes the theoretical development of Causation Entropy, an information-theoretic statistic designed for causality inference. Causation Entropy can be regarded as a type of conditional mutual information which generalizes the traditional, unconditioned version of Transfer Entropy. When applied to Gaussian variables, Causation Entropy also

generalizes Granger Causality and Conditional Granger Causality. We proved that for a general network stochastic process, the causal neighbors of a given node is exactly the minimal set of nodes that maximizes Causation Entropy, a key result which we refer to as the Optimal Causation Entropy Principle. Based on this principle, we introduced an algorithm for causal network inference called Optimal CSE, which utilizes two algorithms to jointly infer the set of causal neighbors of each node.

The effectiveness and data efficiency of the proposed Optimal CSE approach were illustrated through numerical simulation of a Gaussian process on large-scale random networks. In particular, our numerical results show that the proposed Optimal CSE approach consistently outperforms previous Conditional Granger and Transfer Entropy approaches. Furthermore, inference accuracy using the Optimal CSE approach generally requires fewer samples and fewer computations due to its aggregative nature: the conditioning set encountered in entropy estimation remains low-dimensional for sparse networks. The number of samples required for the desired accuracy does not appear to depend on network size, but rather, the density of links (or equivalently, the average degree of the nodes) and spectral radius (which measures the average rate at which information transfers through links). This makes Optimal CSE a promising tool for the inference of networks, in particular large-scale sparse causal networks, as found in a wide range of real-world applications [4, 15, 41, 42].

A few problems remain to be tackled. First, for general stochastic processes, exact expression of entropy is rarely obtainable. Practical application of the Optimal CSE therefore requires the development of non-parametric statistics for estimating Causation Entropy for general multi-dimensional random variables. An ideal estimation method should rely on as few assumptions about the form of the underlying variable as possible and be able to achieve the desired accuracy even for relatively small sample size. Several existing methods, including various binning techniques [53] and k -nearest neighbor estimates [34], seem promising, but further exploration is necessary to examine their effectiveness [27]. Secondly, temporal stationarity assumptions are often violated in real-world applications. It is therefore of critical importance to divide the observed time series data into stationary segments [66], allowing for the inference of causal networks that are *time-dependent* [39]. Finally, information causality suggests physical causality, but they are not necessarily equivalent [27, 46]. It is our goal to put this notion onto a more rigorous footing and further explore their relationships.

Acknowledgments. We appreciate the insightful comments made by I. Ipsen, J. Skufca, G. Song, and C. Tamon. We thank Dr Samuel Stanton from the ARO Complex Dynamics and Systems Program for his ongoing and continuous support.

REFERENCES

- [1] N. A. Ahmed and D. V. Gokhale, Entropy Expressions and Their Estimators for Multivariate Distributions, *IEEE Trans. Inform. Theory* **35**, 688–692 (1989).
- [2] L. Barnett, A. B. Barrett, and A. K. Seth, Granger Causality and Transfer Entropy Are Equivalent for Gaussian Variables, *Phys. Rev. Lett.* **103**, 238701 (2009).
- [3] A. Y. Barraud, A Numerical Algorithm to Solve $AXA - X = Q$, *IEEE Trans. Automat. Control* **22**, 883–885 (1977).
- [4] A. Barrat, M. Barthélemy, and A. Vespignani, *Dynamical Processes on Complex Networks*, (Cambridge University Press, Cambridge 2008).
- [5] B. Bollobás, *Random Graphs* (Academic Press, New York, 2nd ed., 2001).
- [6] E. Bollt, Synchronization as a Process of Sharing and Transferring Information, *Internat. J. Bifur. Chaos Appl. Sci. Engrg.* **22**, 1250261 (2012).

- [7] P. J. Brockwell, *Time Series Analysis: Encyclopedia of Statistics in Behavioral Science* (John Wiley & Sons, Hoboken, New Jersey, 2005).
- [8] D. S. Bassett and E. Bullmore, Small-World Brain Networks, *Neuroscientist* **6**, 512–523 (2006).
- [9] E. Bullmore and O. Sporns, Complex Brain Networks: Graph Theoretical Analysis of Structural and Functional Systems, *Nat. Rev. Neurosci.* **10**, 186–198, (2009).
- [10] N. Chen, On the Approximability of Influence in Social Networks, *SIAM J. Discrete Math.* **23**, 1400–1415 (2009).
- [11] S. P. Cornelius, W. L. Kath, and A. E. Motter, Realistic Control of Network Dynamics, *Nat. Commun.* **4**, 1942 (2013).
- [12] T. M. Cover and J. A. Thomas, *Elements of Information Theory* (John Wiley & Son, Inc., Hoboken, New Jersey, 2nd ed., 2006).
- [13] G. Craciun and M. Feinberg, Multiple Equilibria in Complex Chemical Reaction Networks: Semiopen Mass Action Systems, *SIAM J. Appl. Math.* **70**, 1859–1877 (2010).
- [14] F. Dörfler and F. Bullo, Synchronization and Transient Stability in Power Networks and Nonuniform Kuramoto Oscillators, *SIAM J. Control Optim.* **50**, 1616–1642 (2012).
- [15] S. N. Dorogovtsev, A. V. Goltsev, and J. F. F. Mendes, Critical Phenomena in Complex Networks, *Rev. Modern Phys.* **80**, 1275 (2008).
- [16] M. L. Eaton, *Multivariate Statistics: a Vector Space Approach* (John Wiley and Sons, New York, 1983).
- [17] J. Friedman, T. Hastie, and R. Tibshirani, Sparse Inverse Covariance Estimation with the Graphical Lasso, *Biostatistics* **9**(3) 432–441 (2008).
- [18] Q. Gao, X. Duan and H. Chen, Evaluation of Effective Connectivity of Motor Areas during Motor Imagery and Execution Using Conditional Granger Causality, *NeuroImage* **54**, 1280–1288 (2011).
- [19] I. Gelfand, Normierte Ringe, *Rech. Math. [Mat. Sbornik] N.S.* **9** (51), 3–24 (1941).
- [20] J. W. Gibbs, *Elementary Principles in Statistical Mechanics* (Dover, New York, 1960).
- [21] M. Golubitsky, I. Stewart, and A. Török, Patterns of Synchrony in Coupled Cell Networks with Multiple Arrows, *SIAM J. Appl. Dyn. Syst.* **4**, 78–100 (2005).
- [22] P. Good, *Permutation, Parametric and Bootstrap Tests of Hypotheses* (Springer, 2005).
- [23] C. W. J. Granger, Investigating Causal Relations by Econometric Models and Cross-Spectral Methods, *Econometrica* **37**, 425–438 (1969).
- [24] C. W. J. Granger, Some Recent Developments in a Concept of Causality, *J. Econometrics* **39**, 199–211 (1988).
- [25] G. R. Grimmett and D. R. Stirzaker, *Probability and Random Process* (3rd ed., Oxford University Press, Oxford, UK, 2001).
- [26] S. Guo, A. K. Seth, K. M. Kendrick, C. Zhou, and J. Feng, Partial Granger Causality—Eliminating Exogenous Inputs and Latent Variables, *J. Neuroscience Methods* **172** 79–93 (2008).
- [27] D. W. Hahs and S. D. Pethel, Distinguishing Anticipation from Causality: Anticipatory Bias in the Estimation of Information Flow, *Phys. Rev. Lett.* **107** 128701 (2011).
- [28] J. J. Heckman, Econometric Causality, *Int. Stat. Rev.* **76** 1–27 (2008).
- [29] F. Heider, Social Perception and Phenomenal Causality, *Psychol. Rev.* **51** 358–374 (1944).
- [30] R. A. Horn and C. R. Johnson, *Matrix Analysis* (2nd ed., Cambridge University Press, Cambridge, UK, 2013).
- [31] A. Kaiser and T. Schreiber, Information Transfer in Continuous Processes, *Phys. D* **166**, 43–62 (2002).
- [32] J. Kleinberg, The Small-World Phenomenon: An Algorithmic Perspective, *Proceedings of the 32nd ACM Symposium on Theory of Computing* 163–170 (2000).
- [33] O. Kinouchi and M. Copelli, Optimal Dynamical Range of Excitable Networks at Criticality, *Nat. Phys.* **2**, 348 (2006).
- [34] A. Kraskov, H. Stögbauer, and P. Grassberger, Estimating Mutual Information, *Phys. Rev. E* **69** 066138 (2004).
- [35] O. Kuchaiev, M. Rašajski, D. J. Higham, and N. Pržulj, Geometric De-noising of Protein-Protein Interaction Networks, *PLoS Comput. Biol.* **5**, e1000454 (2009).
- [36] D. B. Larremore, W. L. Shew, and J. G. Restrepo, Predicting Criticality and Dynamic Range in Complex Networks: Effects of Topology, *Phys. Rev. Lett.* **106**, 058101 (2011).
- [37] A. Lasota and M. C. Mackey, *Chaos, Fractals, and Noise: Stochastic Aspects of Dynamics* (2nd ed., Springer-Verlag, New York, 1994).
- [38] S. L. Lauritzen, *Graphical Models* (Oxford University Press, Oxford, UK, 1996).
- [39] A. V. Mantzaris, D. S. Bassett, N. F. Wymbs, E. Estrada, M. A. Porter, P. J. Mucha, S. T. Grafton, and D. J. Higham, Dynamic Network Centrality Summarizes Learning in the Human Brain, *J. Complex Networks* **1** 83–92 (2013).

- [40] W. J. McGill, Multivariate Information Transmission, *Psychometrika* **19**, 97–116 (1954).
- [41] M. E. J. Newman, The Structure and Function of Complex Networks *SIAM Rev.* **45**, 167–256 (2003).
- [42] M. E. J. Newman, *Networks: An Introduction* (Oxford University Press, Oxford, UK, 2010).
- [43] T. Nishikawa and A. E. Motter, Network Synchronization Landscape Reveals Compensatory Structures, Quantization, and the Positive Effect of Negative Interactions, *Proc. Natl. Acad. Sci. USA* **107**(23), 10342–10347 (2010).
- [44] M. Paluš, V. Komárek, Z. Hrnčír, and K. Štěrbová, Synchronization as Adjustment of Information Rates: Detection from Bivariate Time Series, *Phys. Rev. E* **63**, 046211 (2001).
- [45] L. Paninski. Estimation of Entropy and Mutual Information, *Neural Comput.* **15** 1191–1253 (2003).
- [46] J. Pearl, *Causality: Models, Reasoning and Inference* (2nd ed., Cambridge University Press, Cambridge, UK, 2009).
- [47] A. Pomerance, E. Ott, M. Girvan, and W. Losert, The Effect of Network Topology on the Stability of Discrete State Models of Genetic Control, *Proc. Natl. Acad. Sci. USA* **106**, 8209–8214 (2009).
- [48] B. Ravoori, A. B. Cohen, J. Sun, A. E. Motter, T. E. Murphy, and R. Roy, Robustness of Optimal Synchronization in Real Networks, *Phys. Rev. Lett.* **107**, 034102 (2011).
- [49] K. J. Rothman and S. Greenland, Causation and Causal Inference in Epidemiology, *Am. J. Public Health* **95** S144–S150 (2005).
- [50] W. J. Rugh, *Linear System Theory* (Prentice Hall, Englewood Cliffs, NJ, 1993).
- [51] J. Runge, J. Heitzig, V. Petoukhov, and J. Kurths, Quantifying Causal Coupling Strength: A Lag-Specific Measure for Multivariate Time Series Related to Transfer Entropy, *Phys. Rev. Lett.* **108** 258701 (2012).
- [52] J. Runge, J. Heitzig, N. Marwan, and J. Kurths, Escaping the Curse of Dimensionality in Estimating Multivariate Transfer Entropy, *Phys. Rev. E* **86** 061121 (2012).
- [53] K. Hlaváčková-Schindler, M. Paluš, M. Vejmelka, and J. Bhattacharya, Causality Detection Based on Information-Theoretic Approaches in Time Series Analysis, *Phys. Rep.* **441**, 1–46 (2007).
- [54] T. Schreiber, Measuring Information Transfer, *Phys. Rev. Lett.* **85**, 461 (2000).
- [55] C. E. Shannon, A Mathematical Theory of Communication, *Bell System Technical Journal* **27**, 379–423 (1948).
- [56] D. A. Smirnov, Spurious Causalities with Transfer Entropy, *Phys. Rev. E* **87**, 042917 (2013).
- [57] P. Spirtes, C. N. Glymour, and R. Scheines, *Causation, Prediction, and Search* (2nd ed., MIT Press, Cambridge, MA, 2000).
- [58] D. J. Stilwell, E. M. Boltt, and D. G. Roberson, Sufficient Conditions for Fast Switching Synchronization in Time-Varying Network Topologies, *SIAM J. Appl. Dyn. Syst.* **5**, 140–156 (2006).
- [59] G. Stolovitzky, D. Monroe, and A. Califano, Dialogue on Reverse-Engineering Assessment and Methods: the DREAM of high-throughput pathway inference, *Ann. N. Y. Acad. Sci.* **1115**, 1–22 (2007).
- [60] J. Sun and A. E. Motter, Controllability Transition and Nonlocality in Network Control. *Phys. Rev. Lett.* **110**, 208701 (2013).
- [61] J. Sun and E. M. Boltt, Causation Entropy Identifies Indirect Influences, Dominance of Neighbors and Anticipatory Couplings, *Phys. D* **267**, 49–57 (2014).
- [62] D. Taylor and J. G. Restrepo, Network Connectivity during Mergers and Growth: Optimizing the Addition of a Module, *Phys. Rev. E* **83**, 066112 (2011).
- [63] R. Tibshirani, Regression Shrinkage and Selection via the Lasso, *J. R. Stat. Soc. Ser. B Stat. Methodol.* **58**, 267–288 (1996).
- [64] A. L. Traud, E. D. Kelsic, P. J. Mucha, and M. A. Porter, Comparing Community Structure to Characteristics in Online Collegiate Social Networks, *SIAM Rev.* **53**, 526–543 (2011).
- [65] R. Vicente, M. Wibral, M. Lindner, and G. Pipa, Transfer Entropy—a Model-Free Measure of Effective Connectivity for the Neurosciences, *J. Comput. Neurosci.* **30** 45–67 (2011).
- [66] B. Wang, J. Sun, and A. E. Motter, Detecting Structural Breaks in Seasonal Time Series by Regularized Optimization, *Proceedings of the 11th International Conference on Structural Safety and Reliability* (2013, in press).
- [67] D. J. Watts and S. H. Strogatz, Collective Dynamics of ‘Small-World’ Networks, *Nature* **393**, 440–442 (2000).